

4-1-2023

Regulation of astrocyte lipid metabolism and ApoE secretion by the microglial oxysterol, 25-hydroxycholesterol

Anil G Cashikar
Washington University School of Medicine in St. Louis

Danira Toral-Rios
Washington University School of Medicine in St. Louis

David Timm
Washington University School of Medicine in St. Louis

Johnathan Romero
Washington University School of Medicine in St. Louis

Michael Strickland
Washington University School of Medicine in St. Louis

See next page for additional authors

Follow this and additional works at: https://digitalcommons.wustl.edu/oa_4

 Part of the [Medicine and Health Sciences Commons](#)

Please let us know how this document benefits you.

Recommended Citation

Cashikar, Anil G; Toral-Rios, Danira; Timm, David; Romero, Johnathan; Strickland, Michael; Long, Justin M; Han, Xianlin; Holtzman, David M; and Paul, Steven M, "Regulation of astrocyte lipid metabolism and ApoE secretion by the microglial oxysterol, 25-hydroxycholesterol." *Journal of Lipid Research*. 64, 4. 100350 (2023).

https://digitalcommons.wustl.edu/oa_4/2901

This Open Access Publication is brought to you for free and open access by the Open Access Publications at Digital Commons@Becker. It has been accepted for inclusion in 2020-Current year OA Pubs by an authorized administrator of Digital Commons@Becker. For more information, please contact vanam@wustl.edu.

Authors


Anil G Cashikar, Danira Toral-Rios, David Timm, Johnathan Romero, Michael Strickland, Justin M Long, Xianlin Han, David M Holtzman, and Steven M Paul



Regulation of astrocyte lipid metabolism and ApoE secretion by the microglial oxysterol, 25-hydroxycholesterol

Anil G. Cashikar^{1,2,3,4,*}, Danira Toral-Rios¹, David Timm¹, Johnathan Romero¹, Michael Strickland⁴, Justin M. Long^{2,4,5}, Xianlin Han⁶, David M. Holtzman^{2,4,5}, and Steven M. Paul^{1,2,3,4}

¹Department of Psychiatry, ²Hope Center for Neurological Disorders, ³Taylor Family Institute for Innovative Psychiatric Research, ⁴Department of Neurology, and ⁵Knight Alzheimer Disease Research Center, Washington University School of Medicine, St Louis, Missouri, USA; ⁶Barshop Institute for Longevity and Aging Studies, Department of Medicine, University of Texas Health Science Center, San Antonio, Texas, USA

Abstract Neuroinflammation, a major hallmark of Alzheimer's disease and several other neurological and psychiatric disorders, is often associated with dysregulated cholesterol metabolism. Relative to homeostatic microglia, activated microglia express higher levels of *Ch25h*, an enzyme that hydroxylates cholesterol to produce 25-hydroxycholesterol (25HC). 25HC is an oxysterol with interesting immune roles stemming from its ability to regulate cholesterol metabolism. Since astrocytes synthesize cholesterol in the brain and transport it to other cells via ApoE-containing lipoproteins, we hypothesized that secreted 25HC from microglia may influence lipid metabolism as well as extracellular ApoE derived from astrocytes. Here, we show that astrocytes take up externally added 25HC and respond with altered lipid metabolism. Extracellular levels of ApoE lipoprotein particles increased after treatment of astrocytes with 25HC without an increase in *ApoE* mRNA expression. In mouse astrocytes-expressing human ApoE3 or ApoE4, 25HC promoted extracellular ApoE3 better than ApoE4. Increased extracellular ApoE was due to elevated efflux from increased *AbcA1* expression via LXRs as well as decreased lipoprotein reuptake from suppressed *Ldlr* expression via inhibition of SREBP. 25HC also suppressed expression of *Srebf2*, but not *Srebf1*, leading to reduced cholesterol synthesis in astrocytes without affecting fatty acid levels.  We further show that 25HC promoted the activity of sterol-o-acyl transferase that led to a doubling of the amount of cholesteryl esters and their concomitant storage in lipid droplets. Our results demonstrate an important role for 25HC in regulating astrocyte lipid metabolism.

Supplementary key words neuroinflammation • microglia • astrocyte • apolipoprotein E • Alzheimer disease • oxysterols • 25-hydroxycholesterol • cholesterol metabolism

Neuroinflammation is an important hallmark of Alzheimer's disease (AD) and other neurologic diseases as well as certain psychiatric disorders (1). Commonly recognized by the increased numbers of activated microglia and astrocytes in specific regions of the brain, neuroinflammation also entails dramatic changes in gene expression profiles of microglia and astrocytes. In AD, and in mouse models of AD, a specific activated state of microglia is commonly referred to as disease-associated microglia (2–6). The gene expression signature of disease-associated microglia shows downregulation of homeostatic genes and upregulation of several activation markers. One such activation marker is *Ch25h*, encoding cholesterol-25-hydroxylase. Single cell and single nuclei transcriptomics studies show myeloid cell specific overexpression of *Ch25h* in various mouse models of neurological disorders ((7); <http://research-pub.gene.com/BrainMyeloidLandscape/BrainMyeloidLandscape2/#>).

We have recently demonstrated that *Ch25h* is overexpressed in AD brain as well as in mouse models of amyloid deposition and tau-mediated neurodegeneration (8). *Ch25h*, the enzyme that hydroxylates cholesterol to 25-hydroxycholesterol (25HC) (9) is markedly upregulated by toll-like receptor activation of macrophages (10, 11). Activation of primary microglia with the toll-like receptor-4 agonist, lipopolysaccharide (LPS) also upregulates *Ch25h* and results in increased synthesis and release of 25HC into the extracellular milieu (8). 25HC has been shown to have antiviral properties and exhibit context-dependent immunomodulatory effects which can be either proinflammatory or anti-inflammatory (12, 13). While loss of *Ch25h* and 25HC promoted interleukin 1-beta

*For correspondence: Anil G. Cashikar, cashikar@wustl.edu.

production in mouse macrophages (14, 15), 25HC amplified interleukin 1-beta secretion in an ApoE-dependent manner in mouse microglia (8). More recently, we showed that 25HC disrupts hippocampal plasticity and learning in mice (16) suggesting that 25HC may also exhibit neuron-specific activities. These findings illustrate that 25HC not only exhibits autocrine effects on Ch25h-expressing myeloid cells but also supports paracrine effects on neighboring cells.

However, the paracrine effects of 25HC on astrocytes are not well understood. As astrocytes are important for cholesterol synthesis in brain and are a major source of ApoE-containing lipoprotein particles central to cholesterol transport between astrocytes, neurons, and other cells (17), we posited that 25HC released from activated microglia may directly impact lipid metabolism in astrocytes and the secretion of lipoproteins containing ApoE. *APOE* is the most important risk factor for AD and contributes significantly to the risk of developing several other neurological and non-neurological disorders (18). A single copy of the *APOE-E4* allele confers a ~ 3.7 times greater risk than the common variant, *APOE-E3*, whereas homozygous *APOE-E4/E4* carriers have a ~12–15 times greater risk for developing AD. In a mouse model of amyloid deposition, ApoE has been reported to promote the localization of astrocytes to plaques (19). Astrocytes expressing *APOE4* have impaired lipid metabolism and increased accumulation of lipid droplets (LDs) relative to *APOE3*-expressing astrocytes (20–22). ApoE also markedly accelerates amyloid deposition (23, 24) as well as tau-mediated neurodegeneration in mouse models (25). Despite its pathophysiological roles in AD and other CNS diseases, the mechanisms underlying ApoE production and secretion in the brain are not clear. Here, we report that 25HC directly modulates astrocyte lipid metabolism via activation of LXR-mediated and inhibition of SREBP-mediated gene expression as well as by increasing cholesterol esterification. As a result, 25HC promotes extracellular ApoE lipoprotein levels via a posttranslational mechanism. We also show that 25HC exerts a differential effect on extracellular levels of the human ApoE isoforms expressed in mouse astrocytes from human *APOE*-knockin mice. In addition, 25HC enhances esterification of cholesterol and the accumulation of LDs in astrocytes.

MATERIALS AND METHODS

Chemicals

Oxysterols, 5HC (Cayman Chemical Company, 11,097), 25-(C4 Top fluor®)-25HC (Avanti Polar Lipids, 810299P), 7 α 25diHC (Cayman Chemical Company, 11,032), cholesterol (Avanti Polar Lipids, 700,000), LPS (Sigma Aldrich, L2630), GSK2033 (Sigma Aldrich, SML1617), and T0901317 (Cayman Chemical Company 71,810). LY295427 was a kind gift from Dr

Douglas Covey at Washington University School of Medicine, St Louis, MO (26).

Antibodies

Mouse anti-human ApoE monoclonal antibodies (HJ15.7 and biotinylated-HJ15.4; (27)) and mouse anti-mouse ApoE monoclonal antibodies (HJ6.2, HJ6.3, and biotinylated-HJ6.8; (28)) were from the Holtzman lab. Rabbit anti-Abca1 (Novus, NB400-105); Rabbit monoclonal anti-Ldlr (EPI553Y) (Abcam, ab52818); Rabbit anti-ApoJ (Protein Tech, 12289-I-AP); Rabbit anti-Cyp7b1 (Invitrogen, PA5-75380); Mouse anti- β -Actin (Sigma, A5316); Goat anti-rabbit HRP secondary antibody (Leinco Technologies, R115); Goat Anti-rabbit Alexa 555 (Invitrogen, A32732); Goat Anti-mouse Alexa 488 (Invitrogen, A32723).

Mice

Mice lacking *Ch25h* gene were originally developed in the lab of David Russell (10). WT C57BL/6J (referred to as WT) and B6.129S6-*Ch25h*^{tm1Rus}/J (referred to as “*ch25h*-/-” or KO) mice were from Jackson Laboratories (Strain #016263). *APOE* knockin mice with the targeted replacement of the endogenous murine *ApoE* gene with human *APOE- ϵ 3* or *APOE- ϵ 4* were described earlier (29). All mice were maintained on C57BL/6J background and housed in Association for Assessment and Accreditation of Laboratory Animal Care accredited facilities with ad libitum access to food and water on a 12-h light/dark cycle. All animal procedures were approved by the Institutional Animal Care and Use Committee at Washington University and were in agreement with the Association for Assessment and Accreditation of Laboratory Animal Care and WUSM guidelines.

Cells

Primary astrocyte cultures were obtained from the cortex of neonatal mice (2–3 days old). Meninges were removed and cortices dissected in cold Hanks' Balanced Salt solution without calcium and magnesium. The tissue was digested with 0.25% trypsin at 37°C for 5 min and the cell suspension was filtered using a 100 μ m sterile filter. Cells were centrifuged at 300g for 5 min at 23°C and resuspended in astrocyte medium (DMEM + 10% heat-inactivated FBS + 1X Glutamax + 1X Sodium pyruvate and 1X Penicillin/Streptomycin, all from GIBCO). Cells were seeded in a T-75 flask previously coated with 10 μ g/ml poly-D-lysine (Sigma Aldrich, P7280) overnight at 37°C. Cells were cultured for 7–10 days with media changes every 3–4 days to reach a confluent layer of astrocytes. For astrocyte cultures, loosely attached cells microglia were shaken off, followed by trypsinization and replating into desired tissue culture plates at a density of 2×10^5 cells/ml. All treatments were conducted on astrocyte serum-free media (DMEM/Neurobasal (1:1) + 1X Glutamax + 1X Sodium pyruvate + 0.1% of fatty acid-free BSA and 1X penicillin/streptomycin, all were from GIBCO). For 25HC treatment, an identical volume of ethanol was added as Vehicle.

For microglia cultures, the procedure was similar except the culture media also contained 5 ng/ml GM-CSF (GoldBio #1320-03-5) to stimulate microglial proliferation. When large numbers of microglia were observed floating, the flasks were shaken at 200 rpm for 30 min at 37°C. The floating cells were collected by centrifugation and the cells were resuspended in microglia media (DMEM/F12 + 1X Glutamax + 1X Sodium

pyruvate + 0.1% of fatty acid-free BSA and 1× penicillin/streptomycin + 1× insulin, transferrin, and selenite supplement (R&D Systems AR013) + 25 ng/ml M-CSF (GoldBio 1320-09-10). All treatments were done in the same serum-free medium.

Fluorescent 25HC uptake

Cells were seeded at a density of 4×10^4 cells/well in 8-well chambered #1.5 coverglass (CellVis, C8-1.5P). A stock of 2 μ M 25-(C4 Top fluor®)-25HC was prepared in ethanol. Astrocyte treatment media containing 1.8 μ M unlabeled 25HC (90%) and 0.2 μ M TopFluor-25HC (10%) was prepared to result in a total 25HC concentration of 2 μ M. Astrocyte culture media was replaced with treatment media containing 25HC. A kinetic study of 25HC uptake was conducted by fixing cells at 30 min, 1 h, 2 h, 4 h, 1 day with paraformaldehyde (Electron microscopy Sciences, Cat. No. 15710). Cells were counterstained with 4',6-diamidino-2-phenylindole (DAPI) and imaged on Zeiss LSM880 using identical settings at the Washington University Center for Cellular Imaging. Images were processed similarly using ImageJ (Fiji; <https://imagej.net/software/fiji/>).

25HC quantitation

The amount of 25HC released into conditioned culture media by astrocytes and microglia was quantified using previously described methods (30). Briefly, conditioned media was subjected to derivatization with dimethyl glycine followed by liquid chromatography-mass spectrometry. The amount of 25HC was estimated based on an internal standard of deuterated-25HC.

Drug treatments

Mouse primary astrocytes were plated at a density of 2×10^5 cells/ml in a poly-D-lysine coated multiwell plate as needed. Cells were allowed to attach for 2 days, media were removed, and the treatments were diluted in astrocyte serum-free media. Stock solutions of 25HC, cholesterol, T0901317, and LY295427 were made in ethanol and for GSK2033 in DMSO at 10 mM final concentration. 25HC treatments were at 2 μ M final concentration (5000-fold dilution of the stock solution for all experiments). For vehicle control samples, an identical volume of ethanol was added resulting in a final ethanol concentration of 0.02% (~3 mM). For the 25HC concentration series, the highest concentration tested was 4 μ M and corresponding amounts of ethanol as vehicle was used as control. In experiments to test how 25HC influences LXR- and SREBP-pathways, LY295427 and GSK2033 were added to astrocyte serum-free media at a final concentration of 5 μ M. For GSK2033, DMSO was the vehicle control. Treatments were terminated after 1, 2, or 4 days by collecting media and cells for downstream processing as needed.

ApoE ELISA

ELISA for mouse and human ApoE was performed as described earlier (28, 29). The capture antibody was HJ6.2 and HJ15.7, the detection antibody was biotinylated-HJ6.8 and biotinylated HJ15.4 for quantifying mouse and human ApoE, respectively. The ELISA plates were coated with 10 μ g/ml HJ15.7 (human ApoE) or 5 μ g/ml HJ6.2 (mouse ApoE) for 2h at room temperature. The plates were washed with PBS and blocked with 2% BSA in PBS. Samples were diluted appropriately in 1% BSA in PBS with protease inhibitors, loaded into the plates in duplicates, and incubated overnight at 4°C. The

next day, the plates were washed with PBS, followed by addition of the appropriate detection antibody at 50 ng/ml, biotinylated-HJ6.8 (mouse ApoE) or biotinylated HJ15.4 (human ApoE) and incubated for 1 h at room temperature. The plates were washed and incubated with streptavidin-poly-HRP40 (Fitzgerald #65R-S104PHRP) for 1 h at room temperature. The plates were then developed with Super Slow 3,3',5,5'-tetramethylbenzidine (Sigma-Aldrich, Cat# T5569). The development was stopped using 2N sulfuric acid and the plate was read at 450 nm.

Immunoblotting

For secreted proteins, media were collected after the treatment of cells as required. For cellular proteins, cells (treated as appropriate) were washed with PBS and lysed with RIPA buffer (Millipore, Cat. No. 20-188) containing ProBlock Gold™ Mammalian protease inhibitor cocktail (Goldbio, GB-331-1) and Benzonase (Sigma, E1014-5KU). Samples were run on 4–15% Mini protean TGX stain free gels (Biorad, Cat. No.4568085) at 100 V for 1 h. Gels were transferred to PVDF membranes at 100 V by 1 h. Membranes were blocked with a 5% nonfat dry milk in tris-buffered saline with 0.1% Tween-20 (TBST). Primary antibody was diluted in blocking buffer and incubated at 4°C overnight. Blots were washed and incubated with the secondary antibody conjugated to HRP (Leinco Technologies, M114). Blots were developed with chemiluminescent development using Immobilon ECL Ultra Western HRP substrate (Millipore, CS222617) and imaged using the ChemiDoc System (Bio-Rad Labs). Band intensities were quantified using the Image Lab software (Bio-Rad Labs).

ApoE nondenaturing gradient gel electrophoresis

Cells were plated in a 6-well plate with a total density of 4×10^5 cells/well. Supernatants were collected 4 days after treatment. Protein was concentrated from the media using Viva-Spin Turbo 4 (10,000 MWCO) concentrator tubes (Sartorius, VS04T01). Protein samples were run on 4–15% Mini protean TGX stain-free gels (Bio-Rad) at 100 V for 14 h at 4°C. Gels were transferred to PVDF membrane at 100 V for 1 h at 4°C. Immunoblotting was carried out as described above.

Quantitative PCR

RNA was isolated using the Quick-RNA Miniprep Plus Kit (Zymo Research, Cat. No. R1058). cDNA was synthesized from total RNA using High-Capacity cDNA RT kit with RNase inhibitor (Applied Biosystems, Cat No.4374966 Foster City, CA). For the quantitative qPCR (qPCR) reaction mix, PrimeTime probe-based qPCR assays (see Table 1) and PrimeTime Gene Expression Mastermix (Cat. No.1055771) were obtained from Integrated DNA Technologies, Inc. qPCR reactions were run using the Fast mode on a QuantStudio™ 3 Real-Time PCR Instrument (Applied Biosystems by Thermo Fisher Scientific, A28131). For gene expression experiments, data were normalized against actin (*Actb*) and the $2^{-\Delta\Delta C_t}$ method was used to calculate relative gene expression value (Relative Quantity, RQ).

For absolute quantification of *Ch25h* expression in microglia and astrocytes, PrimeTime probe-based qPCR assay for *Ch25h* (Cat. No. Mm.PT.58.42792394.g) from Integrated DNA Technologies was used to determine a standard curve for threshold cycle (C_T) values against the number of copies of *Ch25h* cDNA. Since *Ch25h* is an intronless gene, the plasmid construct with the mouse *Ch25h* gene in pcDNA3.1 (Genscript, OMu18523D) was used to define the standard curve. The C_T

TABLE 1. Probe-based qPCR assays from Integrated DNA Technologies

Mm.PT.58.33540333	<i>ActB</i> , Mus Musculus
PrimeTime Primer 1	ATG CCG GAG CCG TTG TC
PrimeTime Primer 2	GCG AGC ACA GCT TCT TTG
PrimeTime Probe	/56-FAM/CCG CCA CCA /ZEN/GTT CGC CAT G/3IABkFQ/
Mm.PT.58.42792394.g	<i>Ch25h</i> , Mus musculus
PrimeTime Primer 1	CCG ACA GCC AGA TGT TAA TCA C
PrimeTime Primer 2	CGA CCC AAT ACA TGA GCT TCT
PrimeTime Probe	/56-FAM/CGC TGA CCT /ZEN/TCT TCG ACG TGC T/3IABkFQ/
Mm.PT.58.17038655	<i>Cyp7B1</i> , Mus musculus
PrimeTime Primer 1	GGT ACT GGA AAG GGT TCA GAA
PrimeTime Primer 2	AAA CTC TTC AAA GGC AAC ATG G
PrimeTime Probe	/56-FAM/TCC CCA CAA /ZEN/GGA AGA CAG TGA AAG TG/3IABkFQ/
Mm.PT.58.33516165	<i>ApoE</i> , Mus musculus
PrimeTime Primer 1	CAC TCG AGC TGA TCT GTC AC
PrimeTime Primer 2	TGG AGG CTA AGG ACT TGT TTC
PrimeTime Probe	/56-FAM/CCG TGC TGT /ZEN/TGG TCA CAT TGC TG/3IABkFQ/
Mm.PT.58.9651201	<i>Abca1</i> , Mus musculus
PrimeTime Primer 1	CCA TAC CGA AAC TCG TTC ACC
PrimeTime Primer 2	CCG CAG ACA TCC TTC AGA ATC
PrimeTime Probe	/56-FAM/CGT ACG TGC /ZEN/AGA TCA TAG CAA AGA GCT /3IABkFQ/
Mm.PT.58.13959842	<i>Abcg1</i> , Mus musculus
PrimeTime Primer 1	CAT GGT CTT TGC CAG GTA GT
PrimeTime Primer 2	GCT GTT CCT CAT GTT TGC TG
PrimeTime Probe	/56-FAM/CCA GTA GTT /ZEN/CAG GTG CTC CCG G/3IABkFQ/
Mm.PT.58.43082551	<i>Ldlb</i> , Mus musculus
PrimeTime Primer 1	CAT CTA GGC AAT CTC GGT CTC
PrimeTime Primer 2	ATG ACT CAG ACG AAC AAG GC
PrimeTime Probe	/56-FAM/AGT GCA TCT /ZEN/CCC CGC AGT TTG T/3IABkFQ/
Mm.PT.58.8508227	<i>Srebf1</i> , Mus musculus
PrimeTime Primer 1	GTC ACT GTC TTG GTT GTT GAT G
PrimeTime Primer 2	CGA GAT GTG CGA ACT GGA C
PrimeTime Probe	/56-FAM/TGG AGC ATG /ZEN/TCT TCG ATG TCG TTC AA/3IABkFQ/
Mm.PT.58.10032831	<i>Srebf2</i> , Mus musculus
PrimeTime Primer 1	GAC ACA TAA GAG GAT TCG AGA GC
PrimeTime Primer 2	CCC TAT TCC ATT GAC TCT GAG C
PrimeTime Probe	/56-FAM/CCG GTT CAT /ZEN/CCT TGA CCT TTG CGT /3IABkFQ/
Mm.PT.58.11089379	<i>Insig2</i> , Mus musculus
PrimeTime Primer 1	TGG AAG TTG TTG TCG AAG TCT
PrimeTime Primer 2	GCA TTG ACA GGC ATC TAG GAG
PrimeTime Probe	/56-FAM/TTA TAC CCA /ZEN/CGA ACA CCG CCA CG/3IABkFQ/
Mm.PT.58.9805181	<i>Insig1</i> , Mus musculus
PrimeTime Primer 1	ACT CTG AAC CAT GTG CTG AAG
PrimeTime Primer 2	CCC TGA TTT CCT CTA TAT CCG TTC
PrimeTime Probe	/56-FAM/TGT TTC CCA /ZEN/CTG TGA CAC CTC CTG /3IABkFQ/
Mm.PT.58.14276063	<i>Fasn</i> , Mus musculus
PrimeTime Primer 1	ACT CCT GTA GGT TCT CTG ACT C
PrimeTime Primer 2	GCT CCT CGC TTG TCG TC
PrimeTime Probe	/56-FAM/TGG CTC TTC /ZEN/TCT GTC TGG GCT CT/3IABkFQ/
Mm.PT.58.9742054	<i>Acat2</i> , Mus musculus
PrimeTime Primer 1	CTT TAG CTA TTG CCG CAG AC
PrimeTime Primer 2	CCA ATT CCA GCC ATA AAG CAA G
PrimeTime Probe	/56-FAM/AAC AGG TCA /ZEN/ACA TCC TCC AGG GAC /3IABkFQ/
Mm.PT.58.13928402	<i>Hmgcr</i> , Mus musculus
PrimeTime Primer 1	TGC ATG TCA GGA AAG AAC TCC
PrimeTime Primer 2	CCT CTA TAT CCG TTT CCA GTC C
PrimeTime Probe	/56-FAM/CCG TAC CCT /ZEN/TAG AGA TCA TGT TCA TGC C/3IABkFQ/
Mm.PT.58.13417676	<i>Dhcr24</i> , Mus musculus
PrimeTime Primer 1	CGA AGA GGT AGC GGA AGA TG
PrimeTime Primer 2	AGA ACT ACC TGA AGA CAA ACC G
PrimeTime Probe	/56-FAM/CCC TGA GAC /ZEN/ACT ACT ACC ACC GAC A/3IABkFQ/
Mm.PT.58.7525599	<i>Soat1</i> , Mus musculus
PrimeTime Primer 1	GTA TGA TGT AGA GTT CCA CCA GTC
PrimeTime Primer 2	CTG TTC CTT TCG TTC TTT GCC
PrimeTime Probe	/56-FAM/ATG CCT TTG /ZEN/CTG AGA TGT TAC GCT TTG /3IABkFQ/
Mm.PT.58.6537447	<i>Soat2</i> , Mus musculus
PrimeTime Primer 1	CGA AGC TGA AGA GGA GTA AGT C
PrimeTime Primer 2	ACA TTT CCG AAC CAT CTA CCA C
PrimeTime Probe	/56-FAM/TCC AGC ATC /ZEN/AAC CTG CCC TCA T/3IABkFQ/

SOAT, sterol-O-acyl transferase.

values obtained for cDNA prepared from 200 ng RNA isolated from equal number (2×10^5) of microglia or astrocytes were interpolated against the standard curve to determine the absolute number of copies of *Ch25h* in microglia and astrocytes.

Cholesterol efflux assay

To determine how 25HC influences cholesterol efflux, we used the protocol as described earlier (31). Briefly, we first loaded astrocytes for 24 h in the presence of 100 $\mu\text{g}/\text{ml}$ of acetylated LDL from human plasma, (AcLDL, Invitrogen, L35354) previously incubated with 5 μM of Bodipy-cholesterol (Avanti Polar lipids, 810,255) at 37°C for 30 min. Cells were equilibrated in serum-free media for 2 h. To induce cholesterol efflux, cells were incubated with or without 10% mouse serum for 24 h in the presence of 25HC (2 μM) or corresponding vehicle control. After the efflux period media were discarded and cells were washed with 1X PBS and detached using flow cytometry buffer (PBS/2%FBS/1 mM EDTA) for 10 min at 37°C. Cholesterol efflux was assessed directly at a single-cell level by flow cytometry using the Canto II analyzer. Fluorescence in cells without addition of mouse serum indicates “Uptake” and cells with mouse serum stimulation of efflux indicates “Efflux”. Lower levels of cellular fluorescence indicate higher efflux rates.

Lipoprotein reuptake assay

To test how 25HC influences lipoprotein reuptake, we used the LDL Uptake Cell-Based Assay kit (Cayman Chemicals Cat# 10011125) and followed manufacturer instructions. Briefly, we first treated mouse primary astrocytes with vehicle or 2 μM 25HC for 24 h and followed by addition of LDL labeled with DyLight 550 to the culture media for 3 h. At the end of the treatment, cells were washed with cold PBS, fixed with 4% paraformaldehyde, stained with DAPI, and imaged using a microscope. LDL uptake was quantified using ImageJ (Fiji) by normalizing for number of cells (DAPI-positive nuclei) and expressed as LDL sum area per cell.

Lipid droplet analysis

Mouse primary astrocytes were seeded at a density of 3×10^4 cells in a 8-well chamber slide (CellVis, C8-1.5P). Oleic acid was added as Oleic acid-BSA (Sigma O-3008) and used with cell culture BSA (Sigma A-1595) as vehicle control. To address the ability of 25HC to induce LDs, the following treatments were added separately or in combination in astrocyte serum-free media: Vehicle (ethanol + BSA), 25HC (2 μM), oleic acid (30 μM), and the acyl-coenzyme A: cholesterol acyltransferase [sterol-O-acyl transferase (SOAT)] inhibitor, avasimibe (1 μM ; APExBIO cat#A4318). After 24 h, the cells were washed, fixed in 4% paraformaldehyde and stained with BODIPY 493/503 (Thermo Fisher Scientific, D3922) and DAPI. Images from three independent experiments were acquired on the Nikon Spinning Disk Confocal microscope at the Washington University Center for Cellular Imaging. LDs and cells counts were analyzed using ImageJ (Fiji).

Lipidomic analysis

One million astrocytes were grown in six 6-cm dishes and treated with Vehicle or 25HC (2 μM). After 2 days, the media were collected and centrifugated at 4000 rpm \times 5 min to remove cell debris. The cells were washed and collected in

Dulbecco's phosphate buffered saline 1X. Cells were transferred into a microtube and the supernatant was removed after centrifugation at 10,000 $g \times$ 5 min at 4°C. Samples were frozen on dry ice and stored at -80°C . Lipidomic analysis was carried out at the Functional Lipidomics Core at Barshop Institute for Longevity and Aging Studies of the University of Texas Health Science Center, San Antonio, TX. Briefly, lipid extracts of cultured cells were prepared by the procedure of Bligh-Dyer extraction (32) and a premixed solution of internal standards was added based on the protein content of cell homogenates. Individual molecular species of free fatty acids were identified and quantified after derivatization as previously described (33). Total cholesterol and free cholesterol were quantified after derivatization with methoxyacetic acid as described (34). The mass levels of individual cholesterol ester species were calculated from total CE mass and their composition was profiled using precursor-ion scanning of m/z 369. Data processing based on the principles of shotgun lipidomics such as selective ionization, low concentration of lipid solution, and correction for differential isotopologue patterns and kinetics of fragmentation was conducted as previously described (35).

Statistical methods

Means of 2–3 technical replicates for each biological replicate were plotted. To determine statistical significance (P value of <0.05 was considered significant; * 0.05–0.01; **0.01–0.001; *** <0.001). Student's t test or two-way ANOVA with appropriate post hoc multiple comparisons tests (as indicated) were carried out with the help of GraphPad Prism version 9.0 (graphpad.com).

RESULTS

Inflammatory stimuli induce secretion of 25HC in microglia but not astrocytes

Multiple studies reporting single cell-RNAseq data have shown that *Ch25h* is predominantly expressed in microglia in the brain. However, expression of *Ch25h* has also been reported in primary cultured astrocytes (36) and may indicate an altered astrocyte gene expression profile upon isolation and culture. To validate microglia-specific expression of *Ch25h*, we first tested for purity of primary mouse microglia and astrocytes using immunofluorescence with antibodies specific to Iba1 and GFAP (supplemental Fig. S1A, B). While all cells in the microglia culture were positive for Iba1 with no detectable GFAP-positive cells, nearly all cells in the astrocyte cultures were GFAP-positive with only about 1% of Iba1-positive microglia. Next, we measured the expression of *Ch25h* in cultured primary mouse microglia and astrocytes using a qPCR method for absolute quantitation. A standard curve was constructed with C_T value against gene copy number using a known concentration of purified plasmid DNA (pCDNA3.1 with mouse *Ch25h* gene) as shown in supplemental Fig. S1C. Microglia and astrocytes were challenged with 100 ng/ml LPS to stimulate transcription of inflammatory genes including *Ch25h*. Equal amounts of RNA (120 ng) from microglia and astrocytes were used to prepare cDNA for qPCR. The C_T values

for the samples were compared against the standard curve to determine the expression of *Ch25h* between the two cell types. In microglia, *Ch25h* was low in the absence of LPS and increased about 100-fold to 200-fold after treatment with LPS (Fig. 1A). In astrocytes, *Ch25h* was low in the absence of LPS and increased only marginally upon treatment with LPS, presumably resulting from the low levels of contaminating microglia (Fig. 1A).

We next examined the synthesis of 25HC by microglia and astrocytes with or without LPS. Cells were treated with LPS for 24h as before. Conditioned culture media was collected, debris precleared by centrifugation and the media supernatants were subjected to derivatization by dimethyl glycine followed by liquid chromatography and mass spectrometry-based quantitation as described previously (30). While microglia produced high levels of 25HC after LPS treatment, astrocytes produced no appreciable amounts of 25HC with or without LPS (Fig. 1B). High levels of 25HC produced by LPS-treated microglia reflected the high

levels of *Ch25h* expression, demonstrating a causal relationship between *Ch25h* expression and 25HC production in microglia. Therefore, we conclude that inflammatory stimuli triggered overexpression of *Ch25h* and production of 25HC by microglia but not astrocytes. A very low level of *Ch25h* expression could be observed in our primary cultures of isolated neonatal mouse astrocytes most likely due to contaminating microglia. However, no 25HC production and secretion was detected from astrocytes with or without endotoxin stimulus.

It has been suggested that 25HC may be synthesized by enzymes other than *Ch25h* (37). To test this, we examined 25HC synthesis after LPS challenge in microglia from WT and *ch25h*^{-/-} mice (Fig. 1C). Increasing amounts of 25HC as a function of time were observed exclusively in media from WT microglia, whereas no 25HC was detectable in media from *ch25h*^{-/-} microglia. Thus, microglia from *ch25h*^{-/-} mice produce no 25HC as previously demonstrated (8).

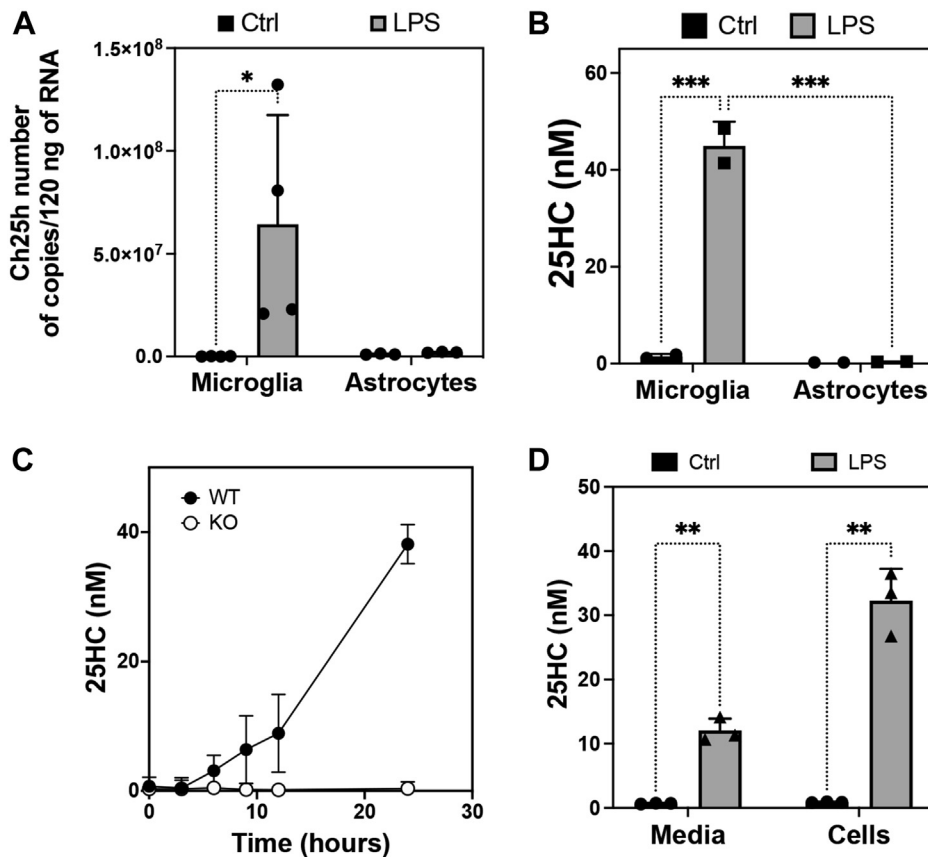


Fig. 1. Microglia express *Ch25h* and secrete 25HC in response to LPS treatment. A: Comparison of *Ch25h* expression between mouse microglia and astrocytes by qPCR in response treatment with 100 ng/ml LPS for 24 h. Data are shown absolute copy numbers of *Ch25h* mRNA per 200,000 cells. A plot of CT values versus copy number is provided in [supplemental Fig. S1](#). (*P*-values, * < 0.05; two-way ANOVA) (B) Measurement of 25HC in conditioned culture media from microglia or astrocytes with or without treatment with 100 ng/ml LPS, as indicated. (*P*-values, *** < 0.0002, Two-way ANOVA with Tukey test for multiple comparisons). C: 25HC production by wildtype (WT) and *ch25h* knockout (KO) microglia was measured in conditioned culture media after treatment with 100ng/ml LPS for various times as indicated. D: Comparison of amount of 25HC in cells versus media at 6 or 24 h after treatment of WT microglia with vehicle (control), 10 ng/ml LPS, or 100 ng/ml LPS. For direct comparison of the distribution of 25HC, cell extracts were prepared in a volume proportional to the volume of media used for cell culture (200,000 cells in 1 ml media). 25HC, 25-hydroxycholesterol; LPS, lipopolysaccharide; qPCR, quantitative qPCR.

We next examined the proportion of 25HC that was secreted into the culture media relative to that retained within microglial cells. To do this, we prepared cell extracts after collecting the conditioned media. The volume of extraction buffer used was equal to the volume of the conditioned culture media to facilitate a direct comparison of 25HC levels. About 30–40% of 25HC produced by microglia after treatment with LPS was released extracellularly into the media while retaining 60–70% of it within cells (Fig. 1D). This distribution is in agreement with that observed earlier for ApoE2- and ApoE4-expressing microglia (8), suggesting that microglial 25HC not only elicit autocrine effects within microglia but may also exert paracrine effects on surrounding cells such as neurons, astrocytes, and other cells to facilitate intercellular crosstalk.

Astrocytes internalize 25HC

To test whether cultured astrocytes could take up and internalize 25HC, astrocytes were treated with 2 μM 25HC mixed with 10% (0.2 μM) BODIPY-labeled fluorescent

25HC (TopFluor-25HC) in culture media, and the uptake of fluorescent 25HC was measured over a period of 24 h (Fig. 2A). Very little fluorescence, if any, could be detected at 2 h. By 4 h, a general increase in fluorescence intensity outlining the cells was visible, suggesting that the 25HC was present in the plasma membrane. By 24 h, 25HC was clearly present in intracellular vesicles in virtually every cell. To confirm whether astrocytes were able to take up unlabeled 25HC added externally into the culture media in the same timeframe, we quantified 25HC remaining in the culture media after 24 h of contact with astrocytes. Interestingly, when astrocytes were treated with 1 μM or 2 μM 25HC, only 44.9 nM (± 1.1 nM) and 84.0 nM (± 8.6 nM) 25HC remained in the conditioned media after 24 h (Fig. 2B). These results suggest that nearly 95% of the externally added 25HC was readily taken up by astrocytes within 24 h.

25HC stimulates ApoE secretion from astrocytes

Since ApoE is a major lipid carrier in the brain produced by astrocytes and its extracellular levels are

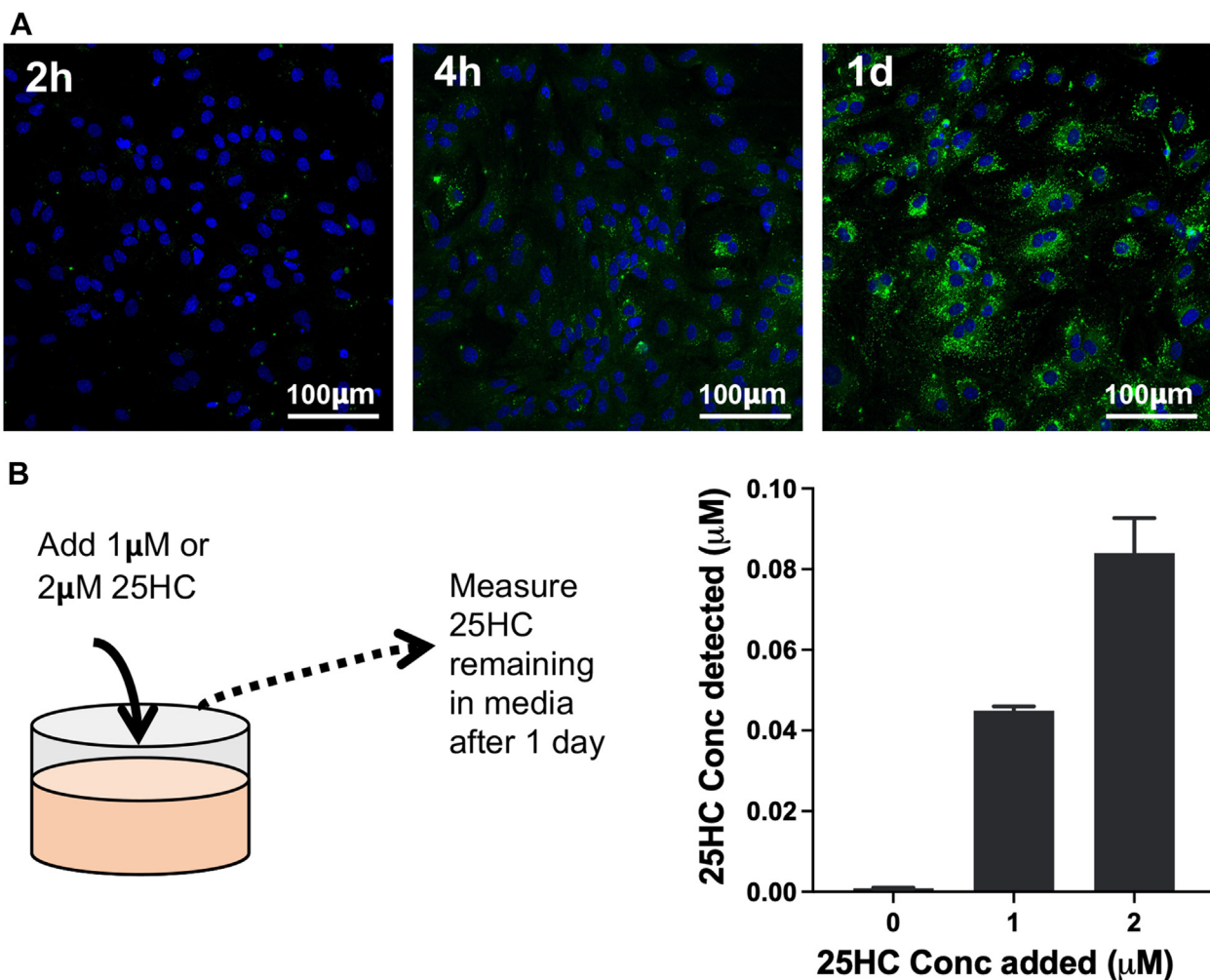


Fig. 2. Uptake of 25HC by astrocytes. A: Fluorescence microscopy of astrocytes treated with 2 μM 25HC (containing 25HC (1.8 μM) and TopFluor-25HC (0.2 μM)) for various times. Time-dependent increase in fluorescence intensity of cells within intracellular vesicles was observed within 1 day B: On the left is a schematic of the experiment showing the addition of 25HC to a final concentration of 1 μM or 2 μM to astrocytes. Uptake of 25HC by astrocytes was monitored using LCMS to measure 25HC remaining (detected) in the culture media after 1 day of incubation on the right. 25HC, 25-hydroxycholesterol.

thought to be central to AD pathogenesis (38), we tested whether 25HC impacts extracellular ApoE from astrocytes. Astrocytes were incubated with 25HC, 7 α 25diHC, cholesterol, T0901317 (a synthetic LXR agonist) or vehicle (ethanol), and the ApoE in the culture media accumulating over 48 h was measured by ELISA (Fig. 3A). While cholesterol or ethanol (vehicle control) had no effect on extracellular ApoE by astrocytes, 25HC increased extracellular ApoE levels by about 200%. The stimulatory effect of 25HC was comparable to an established LXR agonist such as T0901317. Interestingly, 7 α 25diHC, an oxysterol synthesized from 25HC by the enzyme Cyp7b1 also showed no stimulatory effect on extracellular levels of ApoE indicating that the effect of 25HC was not due to its metabolism.

We next tested the effect of 25HC at different concentrations over time. 25HC increased ApoE levels derived from astrocytes in a concentration- and time-dependent manner. At earlier time points (1-day), basal secreted levels of ApoE in conditioned media were low under control conditions and increased by 4-fold to 5-fold over 2 days (Fig. 3B). The amount of extracellular ApoE increased 2-fold to 3-fold following treatment with 25HC (2 μ M) relative to basal levels at both time points.

To better understand the cellular mechanisms responsible for the increased extracellular ApoE in 25HC-treated astrocytes, we isolated RNA from astrocytes treated for 1 day and examined *ApoE* mRNA levels by qPCR. 25HC failed to alter the expression of *ApoE* mRNA at any time. Treatment of astrocytes with vehicle (ethanol) or cholesterol did not alter the expression of *ApoE* mRNA (Fig. 3C). A synthetic nonsteroidal LXR agonist, T0901317, increased *ApoE* mRNA expression by 1.5-fold.

We further examined the amount of ApoE in cell lysates by immunoblotting and compared this with a control protein such as actin B or another apolipoprotein, ApoJ. None of these other astrocytic proteins were altered by 25HC when measured in cell lysates (Fig. 3D). We next tested conditioned media for secreted ApoE and ApoJ. 25HC increased extracellular ApoE but not ApoJ suggesting that the effect was specific for ApoE (Fig. 3E). These observations show that the observed increase in the levels of extracellular ApoE following 25HC treatment occurs without substantially altering intracellular levels of ApoE.

Next, we examined whether the increase in extracellular ApoE by 25HC was associated with an alteration in ApoE quaternary structure. To this end, we concentrated the variously treated conditioned media and separated the secreted ApoE by non-denaturing (native) gel electrophoresis followed by immunoblotting as described previously (29). While each band on the native blot intensified with increasing 25HC concentration, the relative proportions of each of the bands were not different between 25HC-treated and vehicle-treated samples (Fig. 3F). This suggests that the

extracellular ApoE following 25HC treatment of astrocytes was not associated with a change in quaternary structure. Free cholesterol levels in the conditioned media containing ApoE also increased (Fig. 3G) suggesting that the increased extracellular ApoE was lipidated.

To test whether 25HC also increases extracellular levels of human ApoE isoforms, ApoE3 and ApoE4, we treated astrocytes from human APOE knockin mice (29) with various concentrations of 25HC for 48 h. Extracellular human ApoE quantified by ELISA (Fig. 3H) indicated that 25HC strongly promoted an increase of extracellular ApoE3 by 2-fold and 3-fold at 2 μ M and 4 μ M 25HC, respectively. On the other hand, 25HC had a much weaker influence on extracellular ApoE4. Extracellular ApoE4 levels increased marginally at 2 μ M 25HC and by about 1.4-fold by 4 μ M 25HC. Negative stain electron microscopy analyses of ApoE immuno-purified using an antibody specific for human ApoE (HJ15.4) from conditioned culture media of mouse astrocytes expressing human ApoE3 or ApoE4 showed similar lipoprotein particles of about 20 nm diameter for ApoE3 and ApoE4 with or without 25HC (supplemental Fig. S2 and supplemental Table S1) suggesting similar lipidation levels. While the electron micrographs are also suggestive of 25HC-mediated increase in ApoE3- and ApoE4- containing lipoproteins, quantitation of this increase would be inappropriate due to the immuno-isolation step. As in the case of mouse *ApoE* (Fig. 2C), 25HC failed to influence expression of human *APOE3* or *APOE4* in the mouse astrocytes from the human APOE-knockin mice (Fig. 3I) suggesting posttranscriptional control of extracellular ApoE3 and ApoE4.

25HC upregulates *Abca1* and downregulates *LDLR* expression

We next assessed the key genes responsible for ApoE efflux and reuptake by astrocytes by focusing on *Abca1*, which is central to the efflux of ApoE lipoproteins and *Ldlr*, which facilitates its reuptake (39). As a relatively weak ligand of LXRs (40, 41), 25HC may increase the expression of *Abca1*, a gene controlled by LXRs. 25HC is also a strong suppressor of the SREBP-mediated transcription of genes including *Ldlr* (42). By qPCR, we observed that 25HC increased *Abca1* expression after 1 day of treatment by about 2.5-fold ($P < 0.01$), similar to a 3-fold increase observed with the synthetic LXR agonist, T0901317 (Fig. 4A). Vehicle (ethanol) had no significant effect on *Abca1* expression. On the other hand, 25HC strongly suppressed the expression of *Ldlr* to about 10% of control ($P < 0.001$), while treatments with vehicle or T0901317 showed no effect on *Ldlr* expression (Fig. 4B). Similar changes in *Abca1* and *Ldlr* mRNA was observed in mouse astrocytes-expressing ApoE3 and ApoE4 (supplemental Fig. S3), suggesting that differences in the expression of efflux and reuptake genes did not account for the differences in

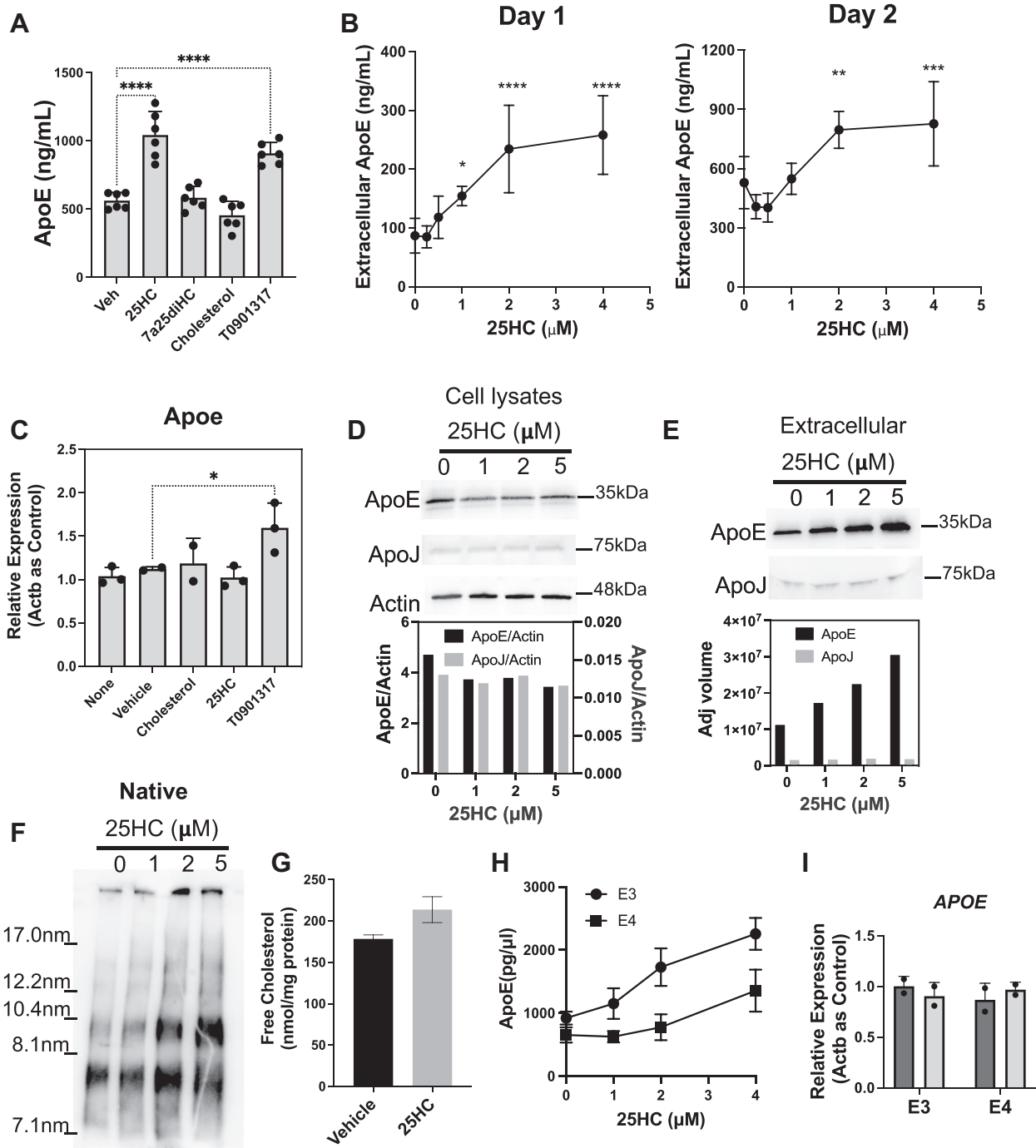


Fig. 3. 25HC increases extracellular ApoE in astrocytes without altering Apoe mRNA expression. A: Astrocytes were incubated with 2 μ M final concentration of 25HC, 7 α 25diHC, cholesterol, T0901317, or with an appropriate amount of vehicle (ethanol). ApoE was measured by ELISA in the conditioned media after 2 days (P -values **** <0.0001 , Two-way ANOVA with Sidak's multiple comparisons test) (B) Effect of 25HC concentration and time on the accumulation of extracellular ApoE from astrocytes. C: Expression of Apoe mRNA was measured by qPCR in astrocytes treated with 2 μ M each of cholesterol, 25HC or T0901317 or an appropriate amount of vehicle (ethanol) or without any treatment (none). Data was normalized to mouse Actb (actin B) as the endogenous control gene and shown as relative expression compared to "None." (*0.05–0.01; One-way ANOVA with Dunnett's multiple comparisons test). D: Immunoblots of cell lysates from astrocytes treated with 0, 1, 2, or 5 μ M 25HC for 48 h. Antibodies for ApoE, ApoJ, or actin are shown on the left of corresponding blots. Bar graphs below the blots show band quantitation after baseline correction normalized for actin band intensity. E: Immunoblots of conditioned media from astrocytes treated with 0, 1, 2, or 5 μ M 25HC for 48 h. Antibodies for ApoE or ApoJ are shown on the left of corresponding blots. Bar graphs below the blots show band quantitation after baseline correction. F: Immunoblot for ApoE of conditioned media from astrocytes treated with 0, 1, 2, or 5 μ M 25HC for 48 h and samples were run on native polyacrylamide gel electrophoresis. G: Extracellular cholesterol in serum-free conditioned media from astrocytes treated with vehicle (black bars) or 2 μ M 25HC (grey bars). H: Extracellular ApoE in mouse astrocytes from knockin mice expressing ApoE3 or ApoE4. I: Expression of APOE was measured by qPCR in astrocytes treated with vehicle (ethanol) or 2 μ M 25HC and normalized to mouse Actb (actin B) (P -values * 0.05–0.01; **0.01–0.001; *** <0.001 ; **** <0.0001 ; Two-way ANOVA with Dunnett's multiple comparisons test). 25HC, 25-hydroxycholesterol; qPCR, quantitative qPCR.

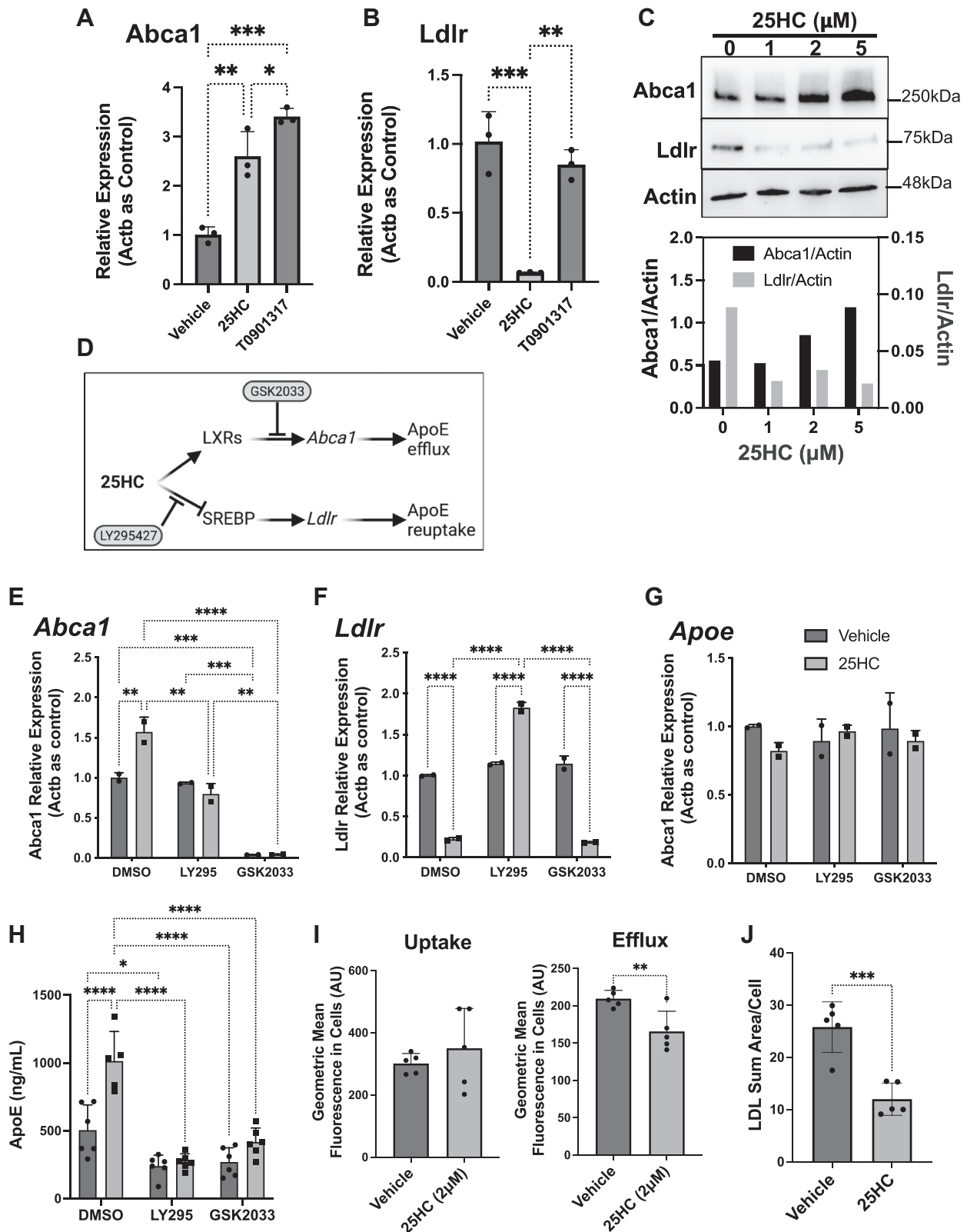


Fig. 4. 25HC increases cholesterol efflux and decreases lipoprotein reuptake. A, B, Expression of *Abca1* (A) and *Ldlr* (B) mRNA in response to treatment of astrocytes with vehicle, 25HC (2 μ M) or T0901317 (2 μ M) was assessed by qPCR. Data is normalized to *Actb* (actin B) as the endogenous control gene and shown as relative expression compared to “vehicle.” (*0.05–0.01; **0.01–0.001; ***<0.001; ****<0.0001; Two-way ANOVA with Sidak’s multiple comparisons test). C: Immunoblots of cell lysates from astrocytes treated with 0, 1, 2, or 5 μ M 25HC for 48 h. Antibodies for Abca1, Ldlr or actin are shown on the left of corresponding blots. Bar graphs below the blots show band quantitation after baseline correction and normalized for actin band intensity. D: Schematic diagram showing the action of inhibitors to block the effect of 25HC on LXR and SREBP pathways. (E, F, and G) Expression of *Abca1* (E), *Ldlr* (F), and *ApoE* (G) mRNA in response to treatment of astrocytes with vehicle or 25HC (2 μ M) in the presence of vehicle (DMSO), 5 μ M LY295427 or

extracellular ApoE3 and ApoE4 (ApoE3 > ApoE4). We confirmed the effects of 25HC on *Abca1* and *Ldlr* mRNA expression by immunoblotting for the respective proteins in mouse astrocytes. In accordance with the mRNA expression levels *Abca1* protein levels increased, while *Ldlr* protein levels decreased following 25HC treatment (Fig. 4C).

25HC-mediated upregulation of LXR-mediated and suppression of SREBP-mediated gene expression are important for ApoE secretion

To determine whether the effects of 25HC on LXR- and SREBP-mediated gene expression are responsible for the increase in extracellular ApoE, we tested the effect of drugs that interfere with each pathway (Fig. 4D). To inhibit the effect of 25HC on the LXR pathway, we treated astrocytes with 25HC in the presence of the LXR antagonist, GSK2033 (43). In the presence of GSK2033, very little expression of *Abca1* was observed with or without 25HC treatment (Fig. 4E) supporting earlier observations that *Abca1* expressed in astrocytes is LXR-dependent. Interestingly, LY295427 reversed 25HC-dependent upregulation of *Abca1* expression (Fig. 4E). Expression of *Ldlr* was suppressed by 25HC as expected and this suppression was unaffected by the presence of GSK2033 (Fig. 4F). To interfere with the 25HC's ability to suppress the SREBP pathway, we tested LY295427, a hypocholesterolemic agent that reduces plasma cholesterol levels by increasing *Ldlr* expression in the liver (44, 45). LY295427 also reversed 25HC-dependent suppression of *Ldlr* expression (Fig. 4F). These effects of LY295427 may be related to the increased expression of *Insig1* as previously observed in cells treated with LY295427 (44).

Neither GSK2033 nor LY295427 had any effect on *ApoE* gene expression (Fig. 4G). However, when the level of ApoE measured in the conditioned media was monitored by ELISA (Fig. 4H), both drugs reduced ApoE levels to about 50% of that of control (vehicle-treated) astrocytes. On the other hand, in the presence of 25HC, both drugs eliminated 25HC-stimulated ApoE levels. These results suggest that interfering with either the LXR pathway or the SREBP pathway eliminates the stimulatory effect of 25HC on extracellular ApoE levels in astrocytes.

25HC modulates efflux and reuptake of ApoE lipoprotein

To determine whether the increased extracellular ApoE resulted from increased efflux (secretion) or from

decreased reuptake of lipoproteins, we examined the effect of 25HC on efflux and uptake of lipoproteins. Towards this goal we first fed astrocytes with BODIPY-labeled cholesterol for 24 h. The cells were treated with vehicle or 25HC together with or without addition of mouse serum as an acceptor of effluxed BODIPY-cholesterol. Fluorescence of BODIPY-cholesterol retained in cells was quantified by flow cytometry. In the absence of mouse serum (termed as "Uptake"), no differences were observed between cells treated with vehicle or 25HC. In the presence of mouse serum as acceptor (termed as "Efflux"), fluorescence within cells decreased significantly after treatment with 25HC compared to vehicle control (Fig. 4I). This suggests that 25HC treatment of cells increased efflux of cholesterol.

Next, to examine how 25HC treatment influences reuptake of lipoproteins as a result of decreased *Ldlr*, we treated astrocytes with vehicle or 25HC for 24 h and allowed them to uptake fluorescently labeled LDL for 4 h. The amount of fluorescence within cells was quantified using microscopy. Treatment of astrocytes with 25HC markedly reduced uptake of labeled LDL relative to vehicle control (Fig. 4J). Together, we conclude that 25HC not only increased ApoE-lipoprotein efflux from astrocytes but also reduced lipoprotein reuptake.

25HC treatment reduces cholesterol biosynthesis in astrocytes

Astrocytes are major producers of cholesterol and other lipids in the CNS. 25HC is a well-characterized oxysterol regulator of the SREBP pathway in peripheral tissues. However, its importance in the CNS has not been studied. We examined how 25HC influences lipid and cholesterol biosynthetic genes in astrocytes compared to a synthetic LXR agonist, T0901317 (Fig. 5A–D). Expression of *Srebf2* (encoding SREBP2, the transcription factor regulating sterol synthesis genes) was reduced to 50% following 25HC treatment of astrocytes for 1 day, whereas T0901317 did not affect *Srebf2* expression (Fig. 5A). Similarly, while 25HC also reduced the expression of *Insig1* (a major regulator of the SREBP pathway) to about 20%, T0901317 marginally increased *Insig1* (Fig. 5B). Interestingly, while 25HC had no effect on the expression of *Srebf1* (encoding SREBP1, the transcription factor regulating fatty acid synthesis genes), T0901317 increased *Srebf1* by about 50% (Fig. 5C). Likewise, while 25HC did not affect the expression of

5 μ M GSK2033 was assessed by qPCR. Data is normalized to *Actb* (actin B) as the endogenous control gene and shown as relative expression compared to "DMSO." (*0.05–0.01; **0.01–0.001; ***<0.001; ****<0.0001; Two-way ANOVA with Sidak's multiple comparisons test). H: ApoE in the conditioned media of astrocytes treated with vehicle or 25HC (2 μ M) in the presence of vehicle (DMSO), 5 μ M LY295427 or 5 μ M GSK2033 was measured by ELISA in the conditioned media after 2 days I: Fluorescence of BODIPY-cholesterol within astrocytes quantified by FACS at the uptake step and the efflux steps after treatment with vehicle (ethanol) or 2 μ M 25HC for 24h. Lower fluorescence within cells indicate higher efflux. J: The amount of TopFluor-LDL uptaken by astrocytes treated with vehicle (ethanol) or 2 μ M 25HC for 24h was measured by microscopy as the fluorescence sum area in the field and normalized to the total number of cells in the field. (*0.05–0.01; **0.01–0.001; ***<0.001; ****<0.0001; Two-way ANOVA with Sidak's multiple comparisons test). 25HC, 25-hydroxycholesterol; qPCR, quantitative qPCR.

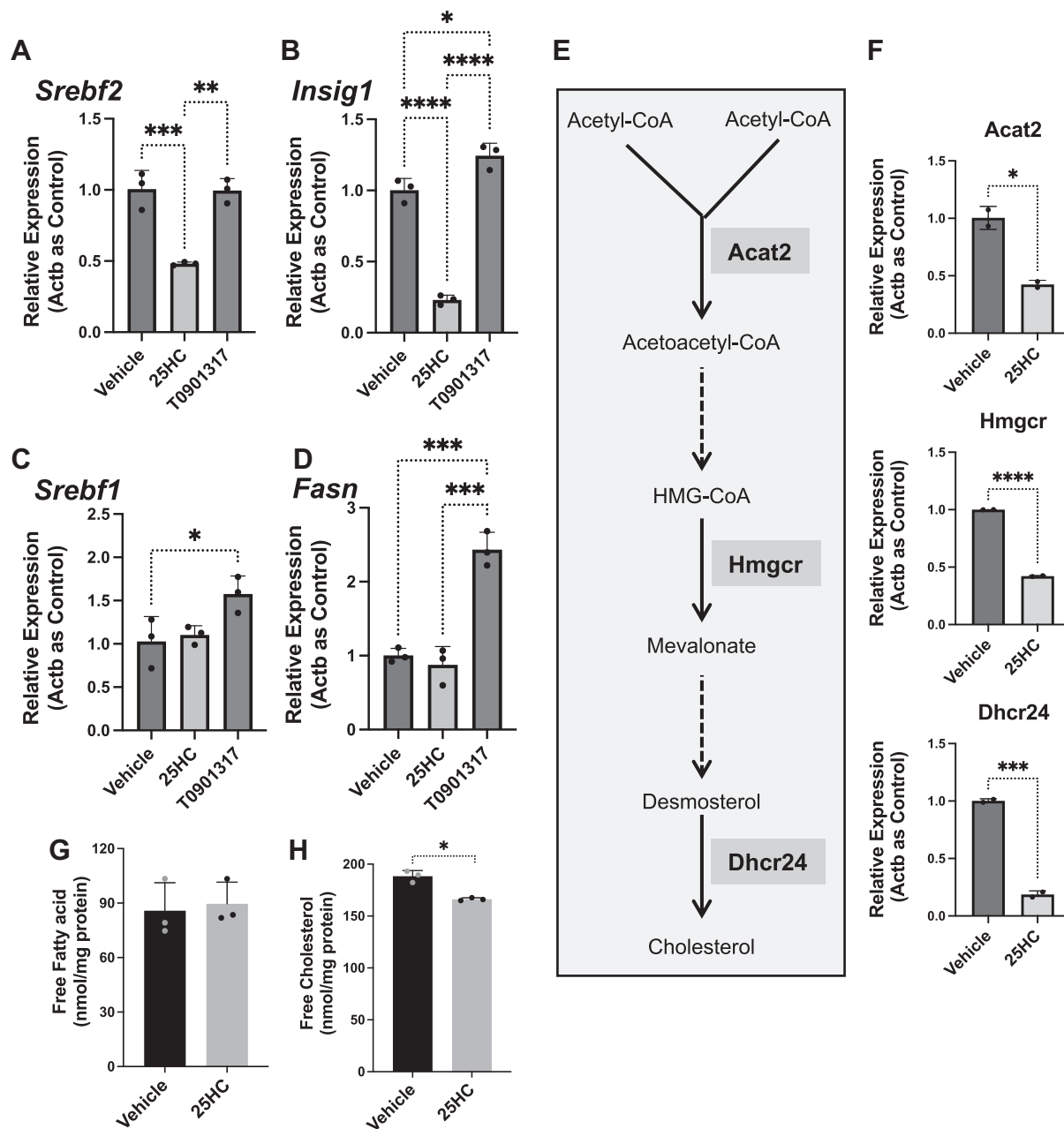


Fig. 5. 25HC suppresses sterol biosynthesis genes in astrocytes. Expression of *Srebf2* (A), *Insig1* (B), *Srebf1* (C), and *Fasn* (D) mRNA in response to treatment of astrocytes with vehicle, 25HC (2 μ M) or T0901317 (2 μ M) for 1 day was assessed by qPCR. Data was normalized to *Actb* (actin B) as the endogenous control gene and shown as relative expression compared to “vehicle”. E: Schematic showing selected steps of cholesterol biosynthesis and the enzyme involved. F: Expression of *Acat2*, *Hmgcr*, and *Dhcr24* in response to treatment of astrocytes with vehicle (black bars) or 2 μ M 25HC (grey bars) for 1 day was quantified by qPCR. Data was normalized to *Actb* (actin B) as the endogenous control gene and shown as relative expression compared to “vehicle”. Quantitation of total free fatty acids (G) and free cholesterol (H) in mouse astrocytes treated with vehicle (black bars) or with 2 μ M 25HC (grey bars). (*0.05–0.01; **0.01–0.001; ***<0.001; ****<0.0001; Two-way ANOVA with Sidak’s multiple comparisons test). 25HC, 25-hydroxycholesterol; qPCR, quantitative qPCR.

Fasn, T0901317 increased *Fasn* by 250% (Fig. 5D). 25HC did not affect the expression of *Srebf1* and *Insig2*.

We next examined the expression of three key genes, namely *Acat2*, *Hmgcr*, and *Dhcr24*, coding for enzymes required for cholesterol biosynthesis as outlined in Fig. 5E. *Acat2* codes for acetyl-coA acyltransferase-2, which catalyzes the first step of cholesterol synthesis.

Hmgcr codes for 3-hydroxy-3-methylglutaryl-coA reductase, an enzyme catalyzing a key step in the synthesis of mevalonate. *Dhcr24* codes for 24-dehydrocholesterol reductase, which catalyzes the last step in cholesterol biosynthesis. The sterol synthesis genes *Acat2*, *Hmgcr*, and *Dhcr24* were markedly decreased after 1 day of treatment with 25HC (Fig. 5F).

Considering the dramatic changes induced by 25HC in cholesterol biosynthesis genes, we next examined whether the changes in gene expression also resulted in corresponding changes in lipids. Astrocytes treated with 25HC or vehicle were tested for changes in free fatty acids (Fig. 5G) and free cholesterol (Fig. 5H). No difference was observed in free fatty acid levels (Fig. 5G) in agreement with a lack of effect of 25HC on *Srebf1* and *Fasn* (Fig. 5C, D). On the other hand, free cholesterol levels were reduced by nearly 10% in 25HC-treated astrocytes relative to vehicle-treated astrocytes (Fig. 5H) reflecting the strong reductions in the expression of *Srebf2* and cholesterol biosynthetic enzymes (Fig. 5E, F).

Augmentation of cholesterol esterification and lipid droplet accumulation by 25HC

Cholesterol ester formation is greatly enhanced by 25HC by the activation of fatty acyl coA:cholesterol acyl transferase enzyme in human fibroblasts (46) and other cells. To determine whether 25HC also enhanced the cholesterol esterification in astrocytes, we examined the intracellular levels of cholesteryl esters (CE) in mouse astrocytes treated with vehicle or 25HC for 24 h. Interestingly, the amount of CE dramatically increased in astrocytes treated with 25HC relative to vehicle (Fig. 6A). Deeper analysis of CE revealed that 25HC significantly increased the amounts of CE14:0, CE16:1, CE16:0, CE18:2, CE18:1, CE20:4, and CE22:5, suggesting that 25HC promoted cholesterol esterification with both saturated as well as mono- or poly-unsaturated fatty acids (Fig. 6B). Previous studies have shown that 25HC activates cholesterol esterification by SOAT (also known as ACAT) (46). We tested whether 25HC also upregulated expression of the two SOATs, *Soat1* and *Soat2*. While 25HC did not affect expression levels (relative to vehicle control) of *Soat1* (Fig. 6C), it increased expression of *Soat2* (Fig. 6D). However, the average C_T values for *Soat2* were very high (>35) suggesting the expression levels were very low. The low *Soat2* expression levels and higher *Soat1* expression levels agree with publicly available databases for expression of these genes in astrocytes in the brain (47).

Since cholesterol esters are mostly stored in LDs, we hypothesized that 25HC might promote LD biogenesis in astrocytes, which has been thought to play an important role in astrocyte function and neuroinflammation (48). To test this, we treated astrocytes with 25HC in the absence or presence of oleic acid (OA), a well-studied fatty acid enhancer of LD biogenesis as well as with avasimibe, an inhibitor of SOAT/ACAT. LDs were detected using BODIPY 493/503 dye which stains neutral lipids (Fig. 6E). In the absence of OA, 25HC increased LD counts in astrocytes and this increase was reversed by avasimibe (Fig. 6E, F) suggesting that the increased CEs in 25HC-treated astrocytes were stored in LDs. OA provides the acyl groups required for the formation of triacylglycerols

from diacyl glycerides as well as for the formation of CEs, which are key neutral lipid components of LDs. Incubation of astrocytes with OA, increased LDs by nearly 10-fold (compare vehicle control in Fig. 6F with OA in Fig. 6G). Interestingly, coincubation of astrocytes with OA and 25HC, nearly doubled the LD content from that resulting from OA alone (Fig. 6E, G). This suggests that in 25HC-treated astrocytes OA further enhanced CEs. While avasimibe had no effect on LDs induced by OA alone, it eliminated the LD-stimulatory effect of 25HC and reverted the levels to that of OA alone. Neither additional of OA nor inhibition of cholesterol esterification by avasimibe altered basal or 25HC-stimulated levels of extracellular ApoE (Fig. 6H). These results suggest that CEs produced in response to treatment of astrocytes with 25HC were stored in LDs but not in ApoE-containing lipoproteins at basal levels as well as when cotreated with an acyl-donor such as OA.

To investigate how 25HC affects LD accumulation in astrocytes expressing human ApoE3 and ApoE4 isoforms, we treated primary astrocytes from knockin mice expressing human *APOE3* or *APOE4* with vehicle or 25HC and examined intracellular LD (supplemental Fig. S4). Contrary to the differential secretion of ApoE lipoproteins between ApoE3- and ApoE4-expressing astrocytes (Fig. 3H), no difference was obvious in LD accumulation between ApoE3- and ApoE4-expressing astrocytes at any concentration of 25HC tested (supplemental Fig. S4).

DISCUSSION

In this study, we have provided evidence that 25HC, a cholesterol metabolite produced almost exclusively by activated microglia alters lipid metabolism in astrocytes (Fig. 7). We have shown that 25HC alters astrocyte lipid homeostasis in various ways including altering cholesterol metabolism, lipoprotein efflux, and reuptake as well as lipid droplet accumulation. Following treatment of mouse astrocytes with physiologically relevant concentrations of 25HC (49), increased secretion as well as decreased reuptake of ApoE lipoproteins resulted in higher levels of extracellular ApoE. Genes required for cholesterol biosynthesis were also strongly downregulated in astrocytes by 25HC. These effects resulted from upregulation of the LXR-mediated gene expression and downregulation of SREBP-mediated gene expression by 25HC. 25HC also led to a marked increase in CE levels and its storage in LDs within astrocytes.

It is unclear whether 25HC is an endogenous ligand for LXRs in vivo. While a recent study showed that 25HC may be an endogenous ligand for LXRs (50), it has been reported to bind LXR weakly (40, 41). However, we have shown that astrocytes readily take up and accumulate 25HC suggesting that the intracellular concentrations of 25HC may be relatively high. Expression of *APOE* is controlled by LXRs (51) in a

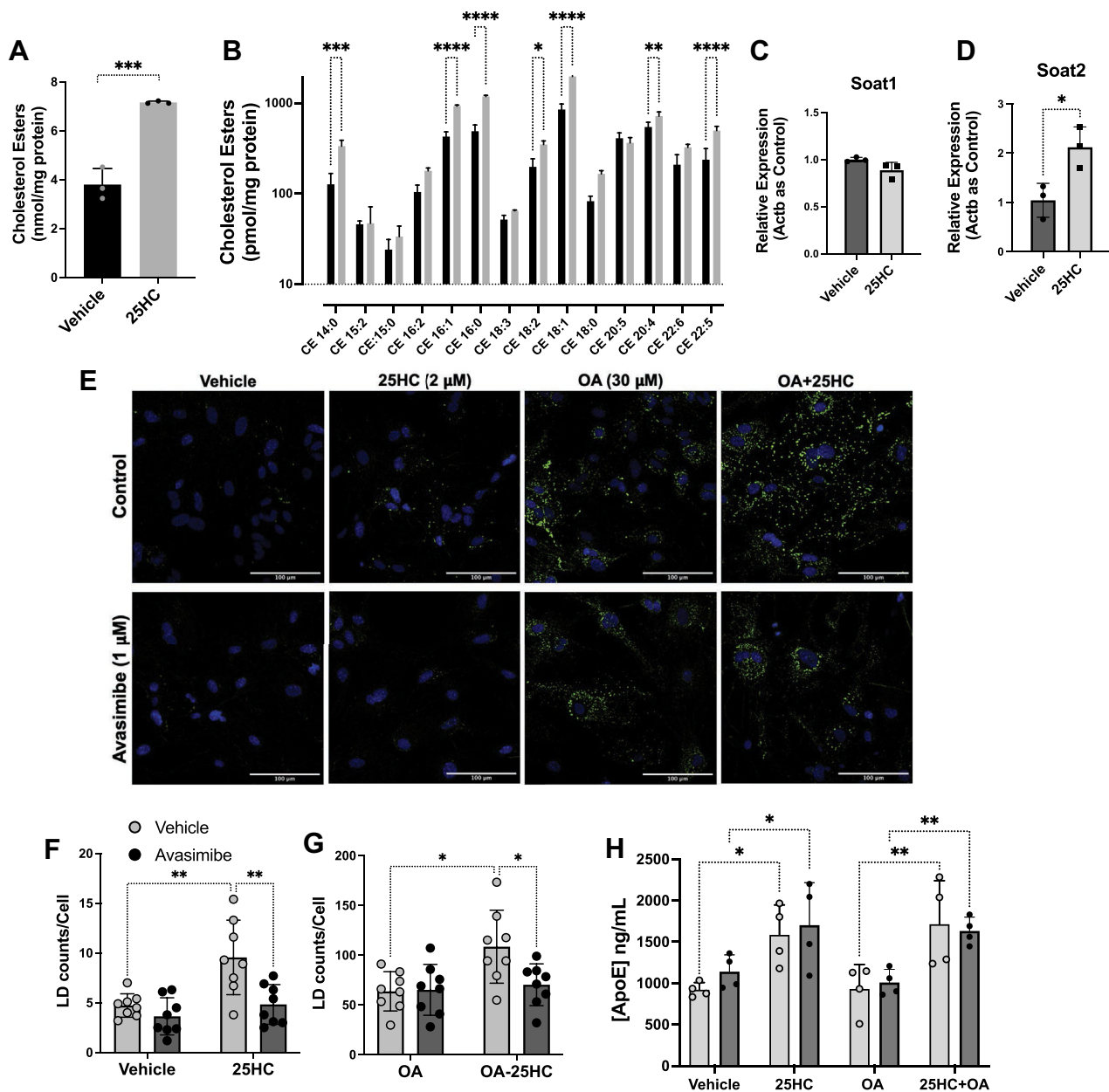


Fig. 6. 25HC increases cholesteryl esters and lipid droplet accumulation in astrocytes. Quantitation of total cholesterol esters (A) in mouse astrocytes treated with vehicle (black bars) or with 2 μ M 25HC (grey bars). Detailed analyses of cholesteryl esters (B) are shown. Expression of *Soat1* (C) and *Soat2* (D) in astrocytes treated with vehicle (black bars) or 2 μ M 25HC (grey bars) was measured by qPCR and normalized to *Actb* as before. E: Mouse astrocytes treated with vehicle (ethanol), 2 μ M 25HC, 30 μ M OA or OA+25HC were stained for lipid droplets with BODIPY (green) and DAPI (blue). Top row of images is without the SOAT/ACAT inhibitor, avasimibe, and bottom row had 1 μ M avasimibe. Bar = 100 μ m. F, G, Quantification of the microscopy data in E and expressed as total LD counts/total nuclei. H, Extracellular ApoE levels quantified by ELISA. Light grey bars are without avasimibe and dark grey bars are with avasimibe. (*0.05–0.01; **0.01–0.001; ***<0.001; ****<0.0001; Data compared with unpaired *t* tests in A. For all others two-way ANOVA with Sidak's multiple comparisons test). SOAT, sterol-O-acyl transferase; LD, lipid droplet; 25HC, 25-hydroxycholesterol; qPCR, quantitative qPCR.

human astrocytoma cell line (CCF-STTG1), where synthetic LXR agonists as well as oxysterols promote ApoE gene expression (52, 53). However, our studies with primary mouse astrocytes show that *ApoE* gene expression is only weakly stimulated by the synthetic LXR agonist, T0901317. Further, *ApoE* expression is neither elevated by 25HC treatment nor inhibited by treatment with the LXR antagonist, GSK2033. Expression of

human *APOE* is also unaffected by 25HC in mouse astrocytes expressing *APOE3* or *APOE4* isoforms. This suggests that expression of mouse *ApoE* mRNA or human *APOE* mRNA does not appear to be strongly dependent on LXRs in mouse astrocytes and in contrary human-derived cells. However, we observed that 25HC significantly increases the expression of *Aba1*, a well-known LXR target gene (54) and that blocking

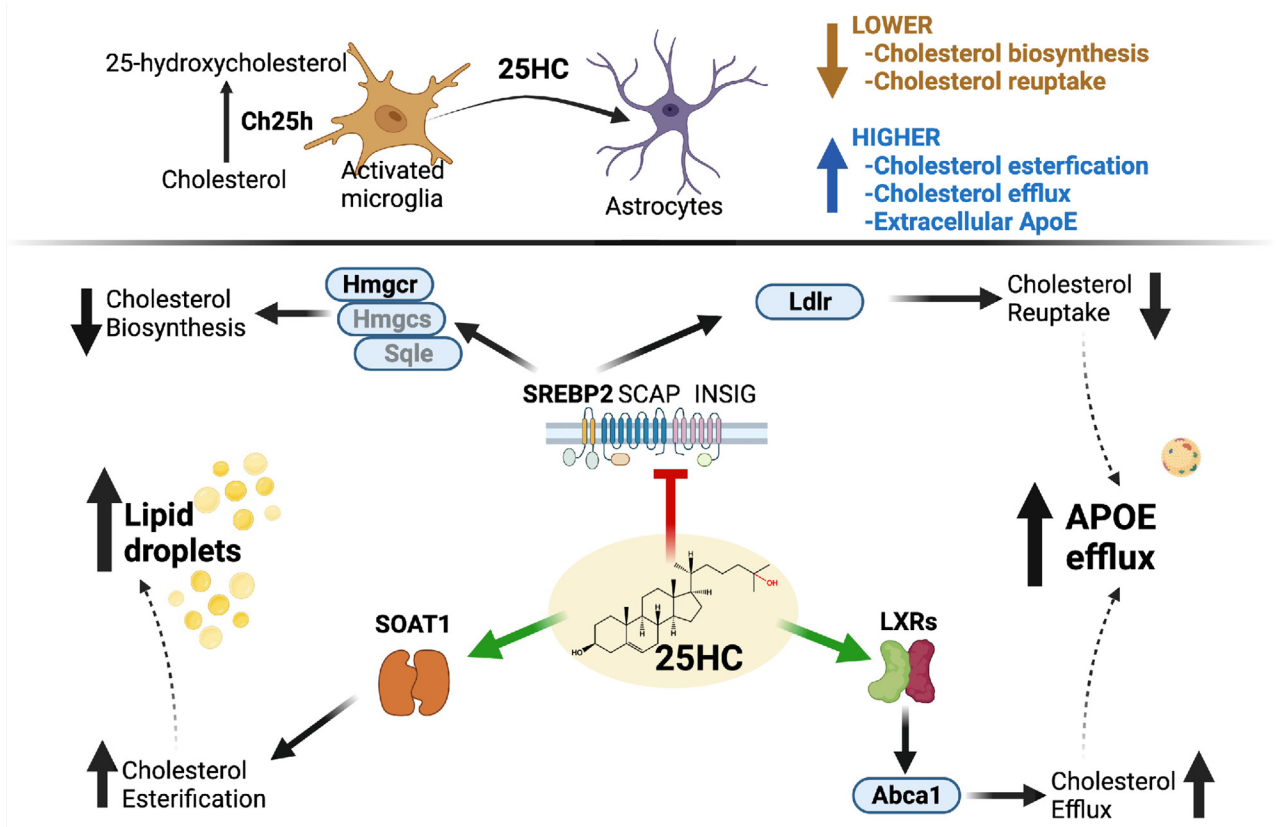


Fig. 7. Lipid metabolism and ApoE secretion in astrocytes is modulated by 25HC, a cholesterol metabolite secreted by activated microglia. **Top:** Overexpression of cholesterol 25-hydroxylase (Ch25h) in microglia activated by inflammatory stimuli converts cholesterol to 25-hydroxycholesterol (25HC). Paracrine effects of secreted 25HC affects astrocyte lipid metabolism and ApoE secretion. **Bottom:** Schematic showing different ways 25HC alters cholesterol metabolism in astrocytes. 25HC inhibits the SREBP2 pathway to suppress cholesterol biosynthesis by reducing the expression of cholesterol biosynthetic enzymes such as Hmgcr. By suppressing LDL-receptor (Ldlr), 25HC also reduces cholesterol reuptake. Activation of LXRs by 25HC promotes expression of Abca1 that increase cholesterol efflux. Decreased reuptake of lipoproteins as well as increased secretion of lipoproteins result in higher levels of extracellular ApoE. Finally, 25HC enhances the activity of the cholesterol acyl transferase enzyme, Acat1 to promote cholesterol esterification. Thus, 25HC effectively reduces free cholesterol in astrocytes. This figure was made using BioRender ([biorender.com](https://www.biorender.com)).

LXR activity with GSK2033 reduced *Abca1* expression in the presence or absence of 25HC. Interestingly, we find that 25HC produced primarily by activated microglia differentially affects extracellular levels of human ApoE3 and ApoE4 without differentially affecting the lipidated form of ApoE or the expression of APOE, *Abca1*, or *Ldlr*. This suggests that the lower extracellular levels of ApoE4-containing lipoproteins relative to ApoE3-containing lipoproteins in response to 25HC treatment may involve other unknown mechanisms.

Astrocytes are a major cell type in the brain for cholesterol biosynthesis, which is controlled by *Srebp2* (42) and may play an important role in the pathogenesis of AD. Cholesterol biosynthesis controlled by the SREBP-pathway encompasses the following key steps: (i) when cholesterol levels are low Scap-Srebp2 complex migrates from the ER to the Golgi via COP-II-dependent trafficking; (ii) in the Golgi Srebp2 is proteolytically cleaved by the S1P and S2P proteases to generate the cytosolic Srebp2 fragment; and (iii) the transcriptionally active Srebp2 fragment translocates to the nucleus to

stimulate transcription of cholesterol synthesis genes. Polymorphisms in the *SREBF2* gene (rs2269657) have been reported to be associated with the risk of developing late onset AD and *SREBF2* mRNA was reported to be significantly higher in AD temporal cortex and cerebellum (55). Astrocyte-derived cholesterol was reported to be important for beta-amyloid production in neurons (56). Further, nuclear Srebp2 has been reported to be negatively correlated with the presence of AT8-positive neurofibrillary tangles in AD brain (57). In mice, astrocyte-specific loss of *Srebp2* resulted in reduced cholesterol synthesis and defects in neurite outgrowth, behavior, and energy metabolism (58). The binding of 25HC to the Insig-Scap interface retains the Scap-Srebp2 complex in the ER precluding its proteolytic processing in the Golgi (59). Treatment of primary astrocytes with 25HC resulted in markedly reduced expression of *Insig1* as well as *Srebp2*, which encodes the Srebp2 protein itself. When 25HC binds to Insig1, it also stabilizes the protein by reducing proteasomal degradation of Insig1 thus promoting its interaction with Scap-Srebp2 (60). Since *Insig1* is a target of the Srebp-

signaling pathway (60), expression of *Insig1* is also reduced in the presence of 25HC. The intricate control of *Insig1* gene expression, protein stability, and function establish a feedback mechanism by which cholesterol biosynthesis is regulated by 25HC.

Following treatment of mouse astrocytes with 25HC, we observed a dramatic decrease in the expression of *Ldlr*, a gene expressed under the control of the SREBP pathway. *Ldlr* is a major receptor for the reuptake of ApoE lipoproteins (61). *Ldlr* is normally localized to the plasma membrane where it binds extracellular ApoE lipoproteins followed by endocytosis and subsequent release of bound lipids in the lysosome (62). Overexpression of LDLR reduced ApoE levels and reduced tau-mediated neurodegeneration (63). On the other hand, by reducing *Ldlr* levels, 25HC markedly limits reuptake of ApoE resulting in greater amounts of extracellular ApoE. A previous study showed that LY295427 reverses the effect of 25HC on the SREBP-pathway by elevating the expression of *Ldlr* (64) as well as *Insig1* (44) presumably by creating a sink for 25HC. In agreement, we observed that 25HC failed to suppress *Ldlr* expression in astrocytes treated with LY295427. However, it is unclear whether LY295427 also reverses the suppression of *Srebf2* expression by 25HC. Taken together, microglial 25HC overproduced under neuroinflammatory conditions may be a potentially important feedback regulator of the SREBP machinery in astrocytes leading to reduced cholesterol biosynthesis as well as lipoprotein reuptake.

25HC also nearly doubled the levels of cholesterol esters and their storage in LDs in astrocytes. Storage and utilization of lipids in LDs in astrocytes are important for astrocyte lipid homeostasis and function (48). Increased LD accumulation in ApoE4-expressing astrocytes has been thought to result from the dysregulation of lipid homeostasis in neuroinflammation (20–22). Our data suggest a role for activated microglia in promoting lipid dysregulation in astrocytes. The increase in 25HC-induced LDs could be blocked by an inhibitor of SOAT/ACAT suggesting the accumulation in CE-rich LDs in 25HC-treated astrocytes. Unlike triglyceride-enriched LDs, CE-enriched LDs are thought to play an important role in the biosynthesis of steroid hormones (65). It will be interesting to examine whether mice lacking *Ch25h* are defective in the production of neurosteroids.

With increased cholesterol efflux, increased cholesterol esterification and decreased cholesterol biosynthesis, the net effect of 25HC on astrocytes is a reduction in overall free cholesterol levels by about 10% in astrocytes as we empirically established. Over long periods, these cholesterol-reducing effects are likely to be detrimental to cell survival.

The results presented herein highlight a potential role for 25HC, the immune-oxysterol produced by microglia to regulate extracellular levels of ApoE as well as cholesterol metabolism in astrocytes. We

postulate that 25HC may function as a potential mediator of microglia-astrocyte crosstalk leading to dysregulation of astrocyte lipid metabolism under conditions of neuroinflammation. It will be interesting to examine the effects 25HC in in vivo models of neuroinflammation and neurodegeneration.

Data availability

All data are contained within the article. 

Supplemental data

This article contains [supplemental data](#) (27, 66, 67).



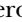




Acknowledgments

We wish to acknowledge the gift of LY295427 from Dr Doug Covey, Department of Developmental Biology, Washington University School of Medicine, St Louis, MO.

Author contributions

A. G. C. and S. M. P. conceived the study; A. G. C., S. M. P. and D. M. H., obtained funding; A. G. C., D. T. R., D. T., J. R., M. S., and X. H., performed experiments; A. G. C., D. T. R., D. T., J. R., M. S., and X. H., analyzed data; D. T. R., J. M. L., D. M. H. and S. M. P., critically reviewed the manuscript; A. G. C., wrote the manuscript

Author ORCIDs

Anil G. Cashikar  <https://orcid.org/0000-0002-3671-684X>
Danira Toral-Rios  <https://orcid.org/0000-0001-5156-6969>
Johnathan Romero  <https://orcid.org/0000-0001-9001-530X>
Michael Strickland  <https://orcid.org/0000-0002-3899-5651>
Justin M. Long  <https://orcid.org/0000-0003-0769-604X>
Xianlin Han  <https://orcid.org/0000-0002-8615-2413>
David M. Holtzman  <https://orcid.org/0000-0002-3400-0856>

Funding and additional information

This research is supported by funding from Centene Corporation contract (P19-00559) for the Washington University-Centene ARCH Personalized Medicine Initiative to A. G. C. and S. M. P. and by a grant from the National Institute on Aging of the National Institutes of Health under Award Number UI9AG069701 (Project 2: A. G. C., S. M. P., and D. M. H. and Core F: X. H.). Support to X. H. for the Functional Lipidomics Core (P30 AG013319 and P30 AG044271) is acknowledged. The content is solely the responsibility of the authors and does not necessarily represent the official views of the National Institutes of Health.

Conflict of interest

S. M. P. is a cofounder, board member and shareholder of Sage Therapeutics, Voyager Therapeutics and Alnylam Pharmaceuticals. He is also a board member and shareholder of Karuna Pharmaceuticals and a Venture Partner at Third Rock Ventures. D. M. H. cofounded and is on the scientific advisory board of C2N Diagnostics. D. M. H. is on the scientific advisory board of Denali and Cajal Neuroscience and consults for Genentech and Alector.

Abbreviations

25HC, 25-hydroxycholesterol; AD, Alzheimer's disease; CE, cholesteryl esters; DAP, 4',6'-diamidino-2-phenylindole; LD, lipid droplet; LPS, lipopolysaccharide; OA, oleic acid; qPCR, quantitative qPCR; SOAT, sterol-O-acyl transferase.

Manuscript received May 3, 2022, and in revised form January 30, 2023. Published, JLR Papers in Press, February 25, 2023, <https://doi.org/10.1016/j.jlr.2023.100350>

REFERENCES

1. Colonna, M., and Butovsky, O. (2017) Microglia function in the central nervous system during health and neurodegeneration. *Annu. Rev. Immunol.* **35**, 441–468
2. Keren-Shaul, H., Spinrad, A., Weiner, A., Matcovitch-Natan, O., Dvir-Szternfeld, R., Ulland, T. K., et al. (2017) A unique microglia type associated with restricting development of Alzheimer's Disease. *Cell*. **169**, 1276–1290.e17
3. Krasemann, S., Madoe, C., Cialic, R., Baufeld, C., Calcagno, N., El Fatimy, R., et al. (2017) The TREM2-APOE pathway drives the transcriptional phenotype of dysfunctional microglia in Neurodegenerative Diseases. *Immunity*. **47**, 566–581.e9
4. Zhou, Y., Song, W. M., Andhey, P. S., Swain, A., Levy, T., Miller, K. R., et al. (2020) Human and mouse single-nucleus transcriptomics reveal TREM2-dependent and TREM2-independent cellular responses in Alzheimer's disease. *Nat. Med.* **26**, 131–142
5. Olah, M., Menon, V., Habib, N., Taga, M. F., Ma, Y., Yung, C. J., et al. (2020) Single cell RNA sequencing of human microglia uncovers a subset associated with Alzheimer's disease. *Nat. Commun.* **11**, 6129
6. Chen, Y., and Colonna, M. (2021) Microglia in Alzheimer's disease at single-cell level. Are there common patterns in humans and mice. *J. Exp. Med.* **218**, e20202717
7. Friedman, B. A., Srinivasan, K., Ayalon, G., Meilandt, W. J., Lin, H., Huntley, M. A., et al. (2018) Diverse brain myeloid expression profiles reveal distinct microglial activation states and aspects of Alzheimer's Disease not evident in mouse models. *Cell Rep.* **22**, 832–847
8. Wong, M. Y., Lewis, M., Doherty, J. J., Shi, Y., Cashikar, A. G., Amelianchik, A., et al. (2020) 25-Hydroxycholesterol amplifies microglial IL-1 β production in an apoE isoform-dependent manner. *J. Neuroinflamm.* **17**, 192
9. Lund, E. G., Kerr, T. A., Sakai, J., Li, W. P., and Russell, D. W. (1998) cDNA cloning of mouse and human cholesterol 25-hydroxylases, polytopic membrane proteins that synthesize a potent oxysterol regulator of lipid metabolism. *J. Biol. Chem.* **273**, 34316–34327
10. Bauman, D. R., Bitmansour, A. D., McDonald, J. G., Thompson, B. M., Liang, G., and Russell, D. W. (2009) 25-Hydroxycholesterol secreted by macrophages in response to Toll-like receptor activation suppresses immunoglobulin A production. *Proc. Natl. Acad. Sci. U. S. A.* **106**, 16764–16769
11. Diczfalusy, U., Olofsson, K. E., Carlsson, A. M., Gong, M., Golenbock, D. T., Rooyackers, O., et al. (2009) Marked upregulation of cholesterol 25-hydroxylase expression by lipopolysaccharide. *J. Lipid Res.* **50**, 2258–2264
12. Diczfalusy, U. (2013) On the formation and possible biological role of 25-hydroxycholesterol. *Biochimie*. **95**, 455–460
13. Cyster, J. G., Dang, E. V., Reboldi, A., and Yi, T. (2014) 25-Hydroxycholesterols in innate and adaptive immunity. *Nat. Rev. Immunol.* **14**, 731–743
14. Reboldi, A., Dang, E. V., McDonald, J. G., Liang, G., Russell, D. W., and Cyster, J. G. (2014) Inflammation. 25-Hydroxycholesterol suppresses interleukin-1-driven inflammation downstream of type I interferon. *Science*. **345**, 679–684
15. Dang, E. V., McDonald, J. G., Russell, D. W., and Cyster, J. G. (2017) Oxysterol restraint of cholesterol synthesis prevents AIM2 inflammasome activation. *Cell*. **171**, 1057–1071.e11
16. Izumi, Y., Cashikar, A. G., Krishnan, K., Paul, S. M., Covey, D. F., Mennerick, S. J., et al. (2021) A Proinflammatory stimulus disrupts hippocampal plasticity and learning via microglial activation and 25-hydroxycholesterol. *J. Neurosci.* **41**, 10054–10064
17. Staurengli, E., Giannelli, S., Testa, G., Sottero, B., Leonarduzzi, G., and Gamba, P. (2021) Cholesterol Dysmetabolism in Alzheimer's Disease: a starring role for astrocytes. *Antioxidants (Basel)*. **10**, 1890
18. Yamazaki, Y., Zhao, N., Caulfield, T. R., Liu, C. C., and Bu, G. (2019) Apolipoprotein E and Alzheimer disease: pathobiology and targeting strategies. *Nat. Rev. Neurol.* **15**, 501–518
19. Koistinaho, M., Lin, S., Wu, X., Esterman, M., Koger, D., Hanson, J., et al. (2004) Apolipoprotein E promotes astrocyte colocalization and degradation of deposited amyloid-beta peptides. *Nat. Med.* **10**, 719–726
20. Farmer, B. C., Kluemper, J., and Johnson, L. A. (2019) Apolipoprotein E4 alters astrocyte fatty acid metabolism and lipid droplet formation. *Cells*. **8**, 182
21. Sienski, G., Narayan, P., Bonner, J. M., Kory, N., Boland, S., Arczewska, A. A., et al. (2021) APOE4 disrupts intracellular lipid homeostasis in human iPSC-derived glia. *Sci. Transl. Med.* **13**, eaz4564
22. Lindner, K., Beckenbauer, K., van Ek, L. C., Titeca, K., de Leeuw, S. M., Awwad, K., et al. (2022) Isoform- and cell-state-specific lipidation of ApoE in astrocytes. *Cell Rep.* **38**, 110435
23. Ulrich, J. D., Ulland, T. K., Mahan, T. E., Nyström, S., Nilsson, K. P., Song, W. M., et al. (2018) ApoE facilitates the microglial response to amyloid plaque pathology. *J. Exp. Med.* **215**, 1047–1058
24. Liu, C. C., Zhao, N., Fu, Y., Wang, N., Linares, C., Tsai, C. W., et al. (2017) ApoE4 Accelerates Early Seeding of Amyloid Pathology. *Neuron*. **96**, 1024–1032.e3
25. Shi, Y., Yamada, K., Liddel, S. A., Smith, S. T., Zhao, L., Luo, W., et al. (2017) ApoE4 markedly exacerbates tau-mediated neurodegeneration in a mouse model of tauopathy. *Nature*. **549**, 523–527
26. Bielska, A. A., Ory, D. S., and Covey, D. F. (2011) Synthesis of the enantiomer of the oxysterol-antagonist LY295427. *Steroids*. **76**, 986–990
27. Liao, F., Zhang, T. J., Jiang, H., Lefton, K. B., Robinson, G. O., Vassar, R., et al. (2015) Murine versus human apolipoprotein E4: differential facilitation of and co-localization in cerebral amyloid angiopathy and amyloid plaques in APP transgenic mouse models. *Acta Neuropathol. Commun.* **3**, 70
28. Kim, J., Eltorai, A. E., Jiang, H., Liao, F., Verghese, P. B., Kim, J., et al. (2012) Anti-apoE immunotherapy inhibits amyloid accumulation in a transgenic mouse model of A β amyloidosis. *J. Exp. Med.* **209**, 2149–2156
29. Huynh, T. V., Wang, C., Tran, A. C., Tabor, G. T., Mahan, T. E., Francis, C. M., et al. (2019) Lack of hepatic apoE does not influence early A β deposition: observations from a new APOE knock-in model. *Mol. Neurodegener.* **14**, 37
30. Jiang, X., Ory, D. S., and Han, X. (2007) Characterization of oxysterols by electrospray ionization tandem mass spectrometry after one-step derivatization with dimethylglycine. *Rapid Commun. Mass Spectrom.* **21**, 141–152
31. Martel, C., Li, W., Fulp, B., Platt, A. M., Gautier, E. L., Westerterp, M., et al. (2013) Lymphatic vasculature mediates macrophage reverse cholesterol transport in mice. *J. Clin. Invest.* **123**, 1571–1579
32. Bligh, E. G., and Dyer, W. J. (1959) A rapid method of total lipid extraction and purification. *Can. J. Biochem. Physiol.* **37**, 911–917
33. Wang, M., Han, R. H., and Han, X. (2013) Fatty acidomics: global analysis of lipid species containing a carboxyl group with a charge-remote fragmentation-assisted approach. *Anal. Chem.* **85**, 9312–9320
34. Cheng, H., Jiang, X., and Han, X. (2007) Alterations in lipid homeostasis of mouse dorsal root ganglia induced by apolipoprotein E deficiency: a shotgun lipidomics study. *J. Neurochem.* **101**, 57–76
35. Wang, M., Wang, C., and Han, X. (2017) Selection of internal standards for accurate quantification of complex lipid species in biological extracts by electrospray ionization mass spectrometry—What, how and why. *Mass Spectrom. Rev.* **36**, 693–714
36. Berghoff, S. A., Spieth, L., Sun, T., Hosang, L., Schlaphoff, L., Depp, C., et al. (2020) Microglia facilitate repair of demyelinated lesions via post-squalene sterol synthesis. *Nat. Neurosci.* **24**, 47–60
37. Diczfalusy, U., and Björkhem, I. (2011) Still another activity by the highly promiscuous enzyme CYP3A4: 25-hydroxylation of cholesterol. *J. Lipid Res.* **52**, 1447–1449
38. Fernández-Calle, R., Konings, S. C., Frontiñán-Rubio, J., García-Revilla, J., Camprubi-Ferrer, L., Svensson, M., et al. (2022) APOE in the bullseye of neurodegenerative diseases: impact of the

- APOE genotype in Alzheimer's disease pathology and brain diseases. *Mol. Neurodegener.* **17**, 62
39. Wahrle, S. E., Jiang, H., Parsadanian, M., Legleiter, J., Han, X., Fryer, J. D., *et al.* (2004) ABCA1 is required for normal central nervous system ApoE levels and for lipidation of astrocyte-secreted apoE. *J. Biol. Chem.* **279**, 40987–40993
 40. Janowski, B. A., Grogan, M. J., Jones, S. A., Wisely, G. B., Kliewer, S. A., Corey, E. J., *et al.* (1999) Structural requirements of ligands for the oxysterol liver X receptors LXRalpha and LXRBeta. *Proc. Natl. Acad. Sci. U. S. A.* **96**, 266–271
 41. Spencer, T. A., Li, D., Russel, J. S., Collins, J. L., Bledsoe, R. K., Consler, T. G., *et al.* (2001) Pharmacophore analysis of the nuclear oxysterol receptor LXRalpha. *J. Med. Chem.* **44**, 886–897
 42. Brown, A. J., Sun, L., Feramisco, J. D., Brown, M. S., and Goldstein, J. L. (2002) Cholesterol addition to ER membranes alters conformation of SCAP, the SREBP escort protein that regulates cholesterol metabolism. *Mol. Cell.* **10**, 237–245
 43. Zuercher, W. J., Buckholz, R. G., Campobasso, N., Collins, J. L., Galardi, C. M., Gampe, R. T., *et al.* (2010) Discovery of tertiary sulfonamides as potent liver X receptor antagonists. *J. Med. Chem.* **53**, 3412–3416
 44. Janowski, B. A. (2002) The hypocholesterolemic agent LY295427 up-regulates INSIG-1, identifying the INSIG-1 protein as a mediator of cholesterol homeostasis through SREBP. *Proc. Natl. Acad. Sci. U. S. A.* **99**, 12675–12680
 45. Janowski, B. A., Shan, B., and Russell, D. W. (2001) The hypocholesterolemic agent LY295427 reverses suppression of tertiary regulatory element-binding protein processing mediated by oxysterols. *J. Biol. Chem.* **276**, 45408–45416
 46. Brown, M. S., Dana, S. E., and Goldstein, J. L. (1975) Cholesterol ester formation in cultured human fibroblasts. Stimulation by oxygenated sterols. *J. Biol. Chem.* **250**, 4025–4027
 47. Zhang, Y., Chen, K., Sloan, S. A., Bennett, M. L., Scholze, A. R., O'Keefe, S., *et al.* (2014) An RNA-sequencing transcriptome and splicing database of glia, neurons, and vascular cells of the cerebral cortex. *J. Neurosci.* **34**, 11929–11947
 48. Lee, J. A., Hall, B., Allsop, J., Alqarni, R., and Allen, S. P. (2021) Lipid metabolism in astrocytic structure and function. *Semin. Cell Dev. Biol.* **112**, 123–136
 49. Griffiths, W. J., and Wang, Y. (2021) Cholesterol metabolism: from lipidomics to immunology. *J. Lipid Res.* **63**, 100165
 50. Madenspacher, J. H., Morrell, E. D., Gowdy, K. M., McDonald, J. G., Thompson, B. M., Muse, G. W., *et al.* (2020) Cholesterol-25-hydroxylase promotes efferocytosis and resolution of lung inflammation. *JCI Insight.* **5**, e137189
 51. Laffitte, B. A., Repa, J. J., Joseph, S. B., Wilpitz, D. C., Kast, H. R., Mangelsdorf, D. J., *et al.* (2001) LXRs control lipid-inducible expression of the apolipoprotein E gene in macrophages and adipocytes. *Proc. Natl. Acad. Sci. U. S. A.* **98**, 507–512
 52. Liang, Y., Lin, S., Beyer, T. P., Zhang, Y., Wu, X., Bales, K. R., *et al.* (2004) A liver X receptor and retinoid X receptor heterodimer mediates apolipoprotein E expression, secretion and cholesterol homeostasis in astrocytes. *J. Neurochem.* **88**, 623–634
 53. Abildayeva, K., Jansen, P. J., Hirsch-Reinshagen, V., Bloks, V. W., Bakker, A. H., Ramaekers, F. C., *et al.* (2006) 24(S)-hydroxycholesterol participates in a liver X receptor-controlled pathway in astrocytes that regulates apolipoprotein E-mediated cholesterol efflux. *J. Biol. Chem.* **281**, 12799–12808
 54. Venkateswaran, A., Laffitte, B. A., Joseph, S. B., Mak, P. A., Wilpitz, D. C., Edwards, P. A., *et al.* (2000) Control of cellular cholesterol efflux by the nuclear oxysterol receptor LXR alpha. *Proc. Natl. Acad. Sci. U. S. A.* **97**, 12097–12102
 55. Picard, C., Julien, C., Frappier, J., Miron, J., Th eroux, L., Dea, D., *et al.* (2018) Alterations in cholesterol metabolism-related genes in sporadic Alzheimer's disease. *Neurobiol. Aging.* **66**, 180.e1–180.e9
 56. Wang, H., Kulas, J. A., Wang, C., Holtzman, D. M., Ferris, H. A., and Hansen, S. B. (2021) Regulation of beta-amyloid production in neurons by astrocyte-derived cholesterol. *Proc. Natl. Acad. Sci. U. S. A.* **118**, e2102191118
 57. Wang, C., Zhao, F., Shen, K., Wang, W., Siedlak, S. L., Lee, H. G., *et al.* (2019) The sterol regulatory element-binding protein 2 is dysregulated by tau alterations in Alzheimer disease. *Brain Pathol.* **29**, 530–543
 58. Ferris, H. A., Perry, R. J., Moreira, G. V., Shulman, G. I., Horton, J. D., and Kahn, C. R. (2017) Loss of astrocyte cholesterol synthesis disrupts neuronal function and alters whole-body metabolism. *Proc. Natl. Acad. Sci. U. S. A.* **114**, 1189–1194
 59. Yan, R., Cao, P., Song, W., Qian, H., Du, X., Coates, H. W., *et al.* (2021) A structure of human Scap bound to Insig-2 suggests how their interaction is regulated by sterols. *Science.* **371**, eabb2224
 60. Gong, Y., Lee, J. N., Lee, P. C., Goldstein, J. L., Brown, M. S., and Ye, J. (2006) Sterol-regulated ubiquitination and degradation of Insig-1 creates a convergent mechanism for feedback control of cholesterol synthesis and uptake. *Cell Metab.* **3**, 15–24
 61. Fryer, J. D., Demattos, R. B., McCormick, L. M., O'Dell, M. A., Spinner, M. L., Bales, K. R., *et al.* (2005) The low density lipoprotein receptor regulates the level of central nervous system human and murine apolipoprotein E but does not modify amyloid plaque pathology in PDAPP mice. *J. Biol. Chem.* **280**, 25754–25759
 62. Brown, M. S., and Goldstein, J. L. (1986) A receptor-mediated pathway for cholesterol homeostasis. *Science.* **232**, 34–47
 63. Shi, Y., Andhey, P. S., Ising, C., Wang, K., Snipes, L. L., Boyer, K., *et al.* (2021) Overexpressing low-density lipoprotein receptor reduces tau-associated neurodegeneration in relation to apoE-linked mechanisms. *Neuron.* **109**, 2413–2426.e7
 64. Bowling, N., Matter, W. F., Gadski, R. A., McClure, D. B., Schreyer, T., Dawson, P. A., *et al.* (1996) LY295427, a novel hypocholesterolemic agent, enhances [3H]25-hydroxycholesterol binding to liver cytosolic proteins. *J. Lipid Res.* **37**, 2586–2598
 65. Shen, W. J., Azhar, S., and Kraemer, F. B. (2016) Lipid droplets and steroidogenic cells. *Exp. Cell Res.* **340**, 209–214
 66. DeMattos, R. B., Rudel, L. L., and Williams, D. L. (2001) Biochemical analysis of cell-derived apoE3 particles active in stimulating neurite outgrowth. *J Lipid Res.* **42**, 976–987
 67. Morikawa, M., Fryer, J. D., Sullivan, P. M., Christopher, E. A., Wahrle, S. E., DeMattos, R. B., *et al.* (2005) Production and characterization of astrocyte-derived human apolipoprotein E isoforms from immortalized astrocytes and their interactions with amyloid-beta. *Neurobiol Dis.* **19**, 66–76